Princetonlaan 6
3584 CB Utrecht
P.O. Box 80015
3508 TA Utrecht
The Netherlands

www.tno.nl

T +31 88 866 42 56
F +31 88 866 44 75

TNO report

TNO 2015 R10755

Recent developments on the seismicity of the Groningen field in 2015

Date	29 mei 2015
Author(s)	Karin van Thienen-Visser, Peter Fokker, Manuel Nepveu, Danijela Sijacic, Jenny Hettelaar, Bart van Kempen
Copy no	
No. of copies	
Number of pages	50 (incl. appendices)
Number of appendices	2
Sponsor	
Project name	F2 - Groningen ondergrond
Project number	060.14108/01.07.03

Summary

Background
On the 17th of January 2014, the minister of Economic Affairs decided to reduce production from five production clusters in the center of the Groningen field to 3 bcm per year for the period 2014 - 2016 in order to try to reduce the seismicity in the center of the field. In addition, total field production was limited to 42.5 bcm for 2014 and 2015 and 40 bcm for 2016 (EZ 2014). Preceding this decision, technical reports (NAM 2013, TNO 2013) concluded that the seismicity is related to the compaction (and hence the production) of the Groningen field.

In 2014 42,41 bcm was produced from the Groningen gas field. Additional reports (TNO 2014a, TNO 2014b) indicated a change in the event density of the field. A decrease in the center of the field was shown as well as slight increases north of Hoogezand and nearby Tjuchem.

Scope
In the beginning of 2015, the Minister of Economic Affairs decided to impose production caps to the Groningen gas production on a semi-yearly basis. For the first six months of 2015 a maximum gas production of 16,5 bcm was allowed. In January 2015 State Supervision of Mines (SSM) advised to reduce production to 39,4 bcm in 2015 and 2016. After a new advice from SSM, which is expected to be presented in June 2015, the definitive production maximum for 2015 will be defined.

In support of their advice of June 1st 2015, State Supervision of Mines has requested the following additional technical evaluations from TNO-AGE:

- An update on the seismicity of the Groningen field
- compaction field based on inversion of subsidence data

Gas production in 2014
In 2014 the total gas production of the Groningen gas field was 42,41 bcm, which is less than the imposed production cap of 42,5 bcm. The Loppersum production clusters (LRM, PAU, POS, OVS, and ZND) produced in total 2,57 bcm in 2014, which is below the production cap of 3 bcm. Production varied over the year, with the majority of gas being produced during the winter months.

Update on the seismicity of the Groningen field 2014/2015

The distribution of higher magnitude (M_L>2) events occurring since September 2014 can be explained by

- The distances to producing clusters vs non-producing clusters which can explain the events close to Appingedam
- The increase of production at the Ten Post cluster (POS) in December 2014

The first explanation would indicate that the effect of reducing production of the Loppersum clusters has been partially overruled by production of other clusters close to Appingedam. The second explanation would indicate that sudden increases in production could lead to a changing pattern of events in time and space. The latter statement cannot yet be proven with statistical significance and should therefore be further evaluated. An analysis of production and seismic events occurring over time could possibly provide further statistical significance.

The observed density of seismic events from April 2014 to April 2015 is different from densities observed during earlier years. Largest seismic event densities are concentrated in the southwest while the center of the field is marked by lower densities. In previous years the density of seismic events in the center were highest in the Groningen field (see also TNO 2014b). This indicates that the reduction of production in the central area has a marked influence on the number of events in the same area. Additionally, there is a striking match of the event density in 2014/2015 to two known fault systems in the field. These fault systems correspond to areas in the field where differential compaction, known to be an indicator for the occurrence of seismic events, exists (Figure ii).

Statistical analysis on the number of seismic events indicates that the number of events per day in the center of the field has halved since January 2014. The southwestern area, however, shows an increase in the number of events per day. Similar to the production, the seismic events of the Groningen fields exhibits clear seasonality with a lag of some two months between production changes and a change in seismic events.

A Bayesian change point model that has been successfully applied in Oklahoma, U.S.A., has also been applied to the Groningen gas field. A change point in the center of the field is found in January 2003. Event rates after 2003 have quadrupled compared to the years prior to 2003. This would indicate that the fault system in the center of the Groningen field has reached criticality in the beginning of 2003, i.e. small changes in stress will lead to seismic events. Over the whole of the field change points are identified which vary in time (from 2003 to 2010); the earliest times in the center of the field and later times at the edges of the field. This corresponds to the observation that events have started to occur in the center of the field and have spread in time over the field. If the change point indicates when a fault system becomes critical then this also means that different fault systems have become critical at different times.

After 2009 no change point in the center of the field has been found for seismic events with magnitudes larger than M_L=1.5. The number of events (ML≥1.5) since 2014 is probably not enough to show a change point in event rates. Thus this data cannot be used to prove statistically significant changes in event rates since the production reduction of January 2014.

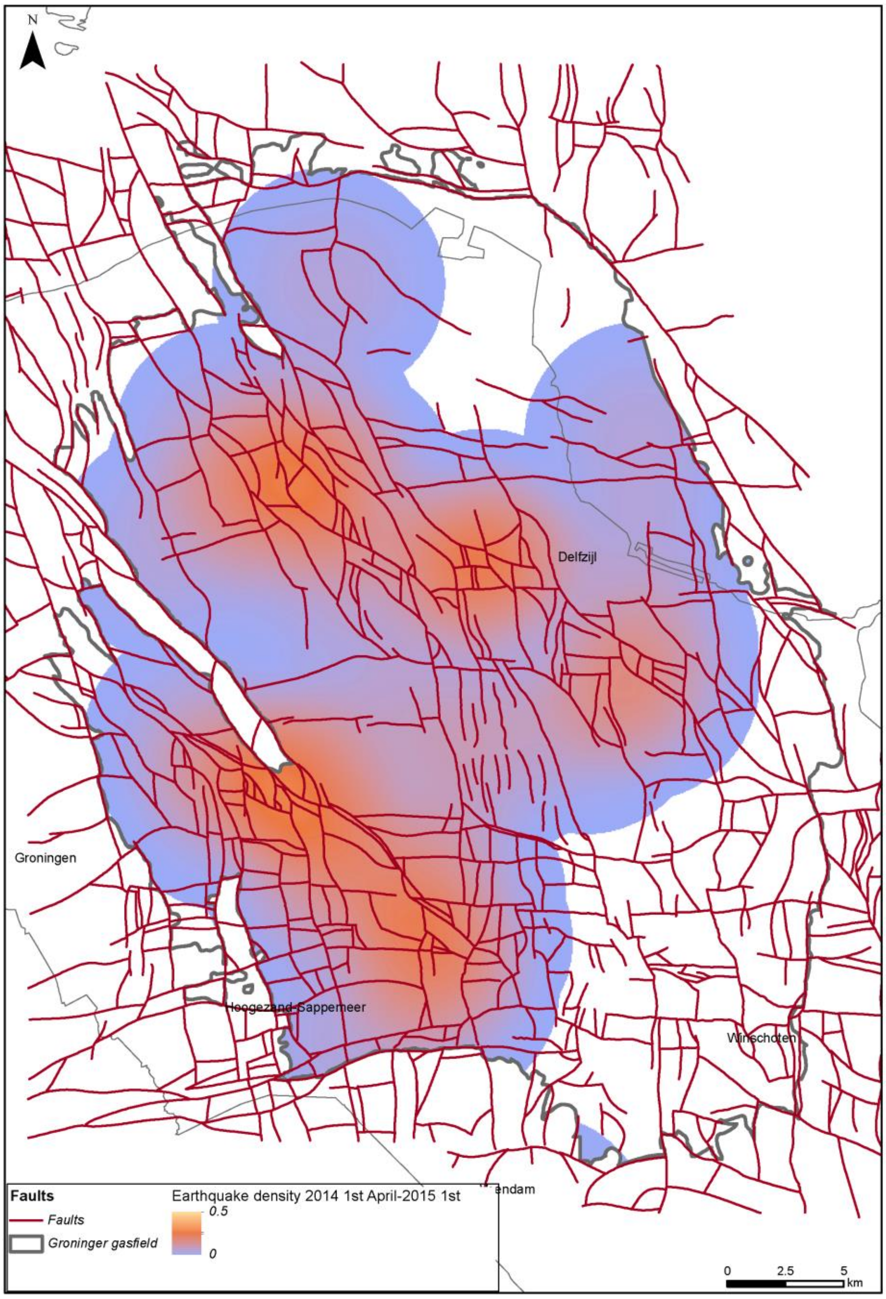


Figure i. Event density (number of events per km^2) from April 1st 2014 to April 1st 2015 shown with the faults in the reservoir (dark red) and the contour of the field (dark blue).

Alternative compaction field

Inversion of subsidence data has provided a correction to the compaction field presented in TNO (2013, 2014a,b). The correction is predominantly applied in regions where previously erroneous porosity estimations or aquifer activity were suspected. The area of maximum compaction has shifted to the west and does not correspond to the area of maximum event density in the center of the field. This indicates that in this regard the presence of faults is more important for seismicity

than the compaction itself. Also differential compaction, known to be an indicator for the occurrence of seismicity, is visible over faults.

This leads to the conclusion that the existing seismological model which NAM has used in the production plan (NAM, 2013), based on an empirical relation between total compaction and the occurrence of events, needs to be updated. As indicated in TNO (2013, 2014a,b) the faults in the reservoir play an important role in the occurrence of events within the field and therefore they have to be taken into account in any future seismological model.

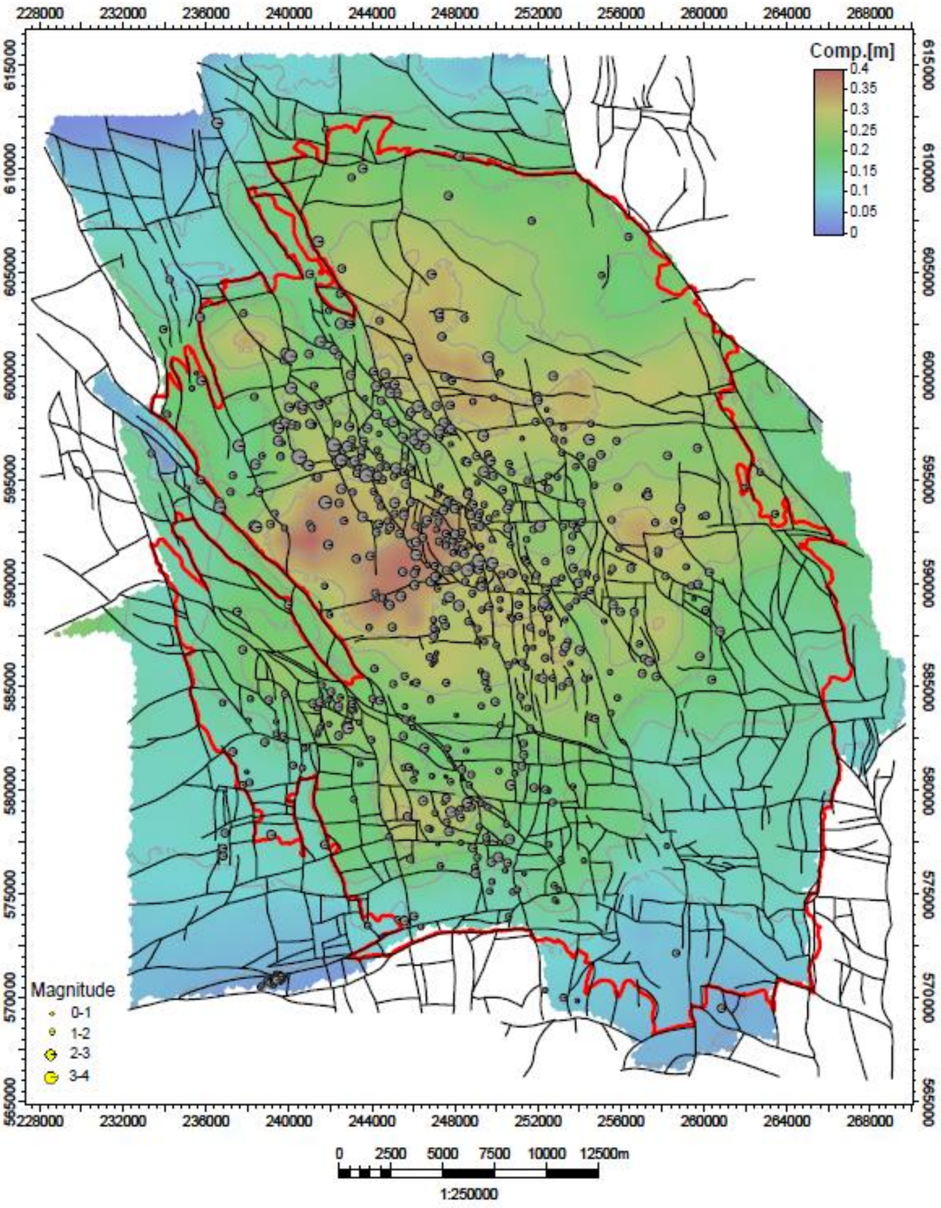


Figure ii. Compaction (m) in 2013 obtained through inversion of subsidence measurements. The red line shows the contour of the Groningen field and the black lines are the faults that are present in the geological model in Petrel (NAM, 2013). Also shown is the seismicity in the field, the size of the symbols indicates the magnitudes of the events

Contents

Figures

Tables

1 Introduction

Background

On the 17th of January 2014, the minister of Economic Affairs decided to reduce production from five production clusters in the center of the Groningen field to 3 bcm per year for the period 2014 - 2016 in order to try to reduce the seismicity in the center of the field. In addition, total field production was limited to 42.5 bcm for 2014 and 2015 and 40 bcm for 2016 (EZ 2014). Preceding this decision, technical reports (NAM 2013, TNO 2013) concluded that the seismicity is related to the compaction (and hence the production) of the Groningen field.

In 2014 42,41 bcm was produced from the Groningen gas field. Additional reports (TNO 2014a, TNO 2014b) indicated a change in the rate of seismicity in the field. A decrease in the center of the field was shown as well as slight increases north of Hoogezand (southwest area) and nearby Tjuchem (eastern area).

Scope

In the beginning of 2015, the Minister of Economic Affairs decided to impose production caps to the Groningen gas production on a semi-yearly basis. For the first six months of 2015 a maximum gas production of 16,5 bcm was allowed. In January 2015 State Supervision of Mines (SSM) advised to reduce production to 39,4 bcm in 2015 and 2016. After a new advice from SSM, which is expected to be presented in June 2015, the definitive production maximum for 2015 will be defined.

In support of their advice, State Supervision of Mines has requested the following additional technical evaluations from TNO-AGE:

- An update on the seismicity of the Groningen field
- compaction field based on inversion of subsidence data

Report setup

Chapters 2 and 3 report the key results and findings of TNO’s evaluations.
In chapter 2 the seismicity of the Groningen field since January 2014 is reported including statistical analysis on observed seismic events. Chapter 3 presents the compaction field l based on the inversion of subsidence data and its implications for the link between compaction, seismicity and the existing faults in the reservoir. Finally, chapter 4 summarizes the findings from chapters 2 and 3 with regards to the questions of SSM.

2 Recent developments of the events in 2014 and 2015

2.1 Introduction

On January 17th 2014 a reduction of production was imposed on the Groningen gas field. As a part of this overall reduction, the production in the five clusters in the center of the field (clusters Leermens (LRM), Ten Post (POS), de Paauwen (PAU), Overschild (OVS), 't Zandt (ZND); see Figure 2-1) was reduced to 3 bcm per year.

TNO (2013) and NAM (2013) concluded that seismicity in the field is linked to compaction, and compaction on its turn is directly linked to production. Hence the observed rate of seismic events (number of events per unit time and unit area) should be indicative for whether the decrease in production has had an effect on seismicity since the implementation of the production reduction measures.

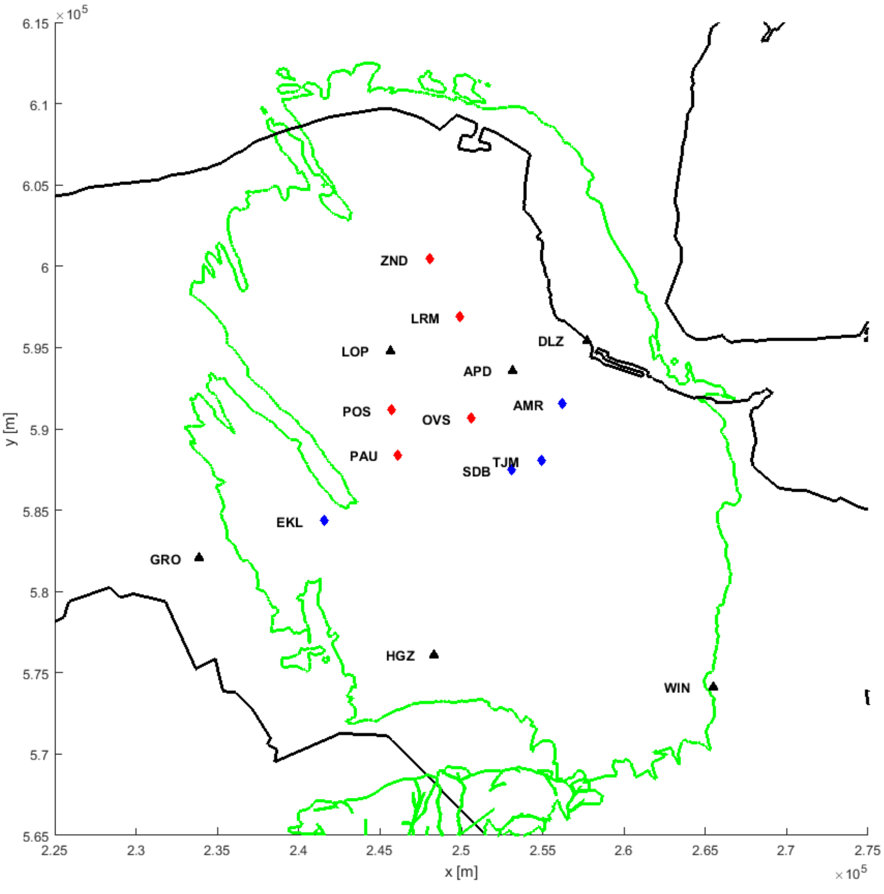


Figure 2-1. Overview of the mentioned clusters: the Loppersum clusters (LRM, PAU, POS, OVS, ZND); the clusters close to Appingedam (AMR, SDB, TJM) and Eemskanaal (EKL). Additionally a few cities are indicated (GRO=Groningen, HGZ= Hoogezand, WIN=Winschoten, DLZ= Delfzijl, LOP=Loppersum, APD=Appingedam). The contour of the Groningen gas field and the Annerveen gas field to the south is indicated in green, the topography in black.

This chapter presents an update on chapter 2 of TNO (2014b) regarding the event densities. In section 2.2 the production of the field in 2014 is presented, in section 2.3 the observed seismic events in 2014 and 2015 above magnitude M_L=2.0 are discussed. In section 2.4 the event density from April 1st 2014 to April 1st 2015 is shown. The event densities are compared to the observed event densities for the same period in the previous years in section 2.5. Section 2.6 describes the statistics of the induced seismicity in a Bayesian analysis and an analysis for seasonality of the events. Finally in section 2.7 a Bayesian Point Change model is applied to the induced events.

2.2 Gas Production of the Groningen field

With 42,41 bcm of gas produced in 2014, the total production of the Groningen field stayed below the imposed production cap of 42,5 bcm. The so-called Loppersum clusters (LRM, PAU, POS, OVS, ZND) produced in total 2,57 bcm in 2014 (see Table 2-1), which is also below the imposed production cap of 3 bcm/yr. Production varied over the year and was highest during the winter months (Figure 2-2).

Table 2-1. Production in 2014 of the five Loppersum clusters.

Cluster	Production in 2014 (bcm)
LRM	0.57
PAU	0.28
POS	0.61
OVS	0.62
ZND	0.49

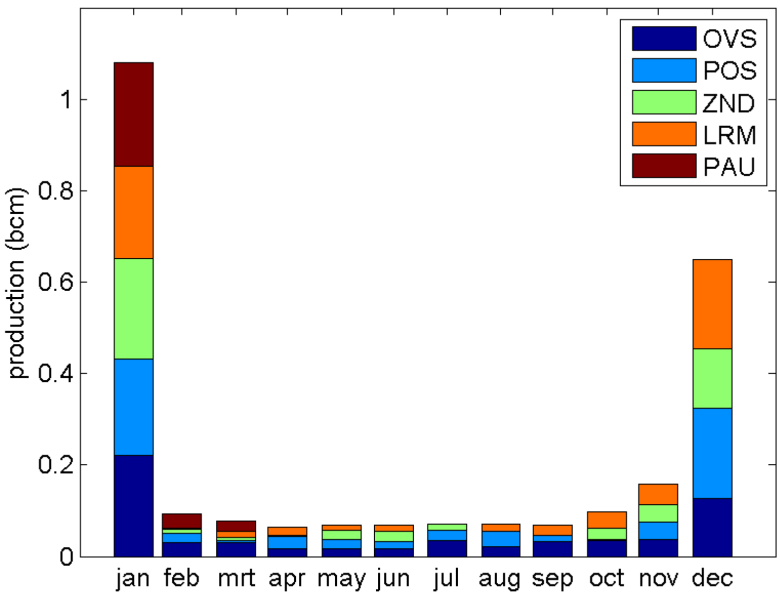


Figure 2-2. Production (taken from www.nlog.nl) of the five Loppersum clusters: Leermens (LRM), Overschild (OVS), De Paauwen (PAU), Ten Post (POS), ‘t Zandt (ZND) in 2014 indicated per month.

2.3 Induced Seismicity of the Groningen field in 2014/2015, events larger than M_L=2

Table 2-2 shows the events with magnitudes larger than M_L=2 that have occurred in Groningen since September 2014. This date has been chosen as the production reduction in Loppersum will have influenced part of the field in the center (TNO 2014a,b), influencing the number and possibly magnitude of the events. The underlying assumption here is the pressure diffusion model, which was presented in TNO (2014b).

Table 2-2. Induced seismicity (taken from www.knmi.nl) of the Groningen field, events larger than M_L=2 and after September 2014.

Event	date	M_L
Garnerwolde	30-09-2014	2.8
Zandeweer	05-11-2014	2.9
Woudbloem	30-12-2014	2.8
Wirdum	06-01-2015	2.7
Appingedam	25-02-2015	2.3
Appingedam	24-03-2015	2.3

The events in Garnerwolde and Woudbloem occurred in the southwest region of the field, not affected by the production reduction in the center. In TNO (2014b) the southwest region is described in more detail.

The Zandeweer event occurred in the north of the field. This part of the field has not yet been influenced by the production reduction of the Loppersum clusters as the travel speed of the pressure is influenced by the permeability of the reservoir (for details see TNO, 2014b).
The two events near Appingedam both occurred in 2015. These events occurred close to the production clusters Amsweer (AMR), Siddeburen (SDB) and Tjuchem (TJM) as well as to the Loppersum clusters Overschild (OVS) and Leermens (LRM) (Figure 2-1). The increase of events near Appingedam may indicate that the pressure wave associated with the continuing production in the nearby clusters of AMR, SDB and TJM causes compaction and consequently seismicity in that area. It is, however, too early to draw conclusions from this statement and more observations are needed to support statistical significance.

The event near Wirdum occurred in the Loppersum area in the beginning of January 2015. With a distance of 2.1 km the POS cluster is the nearest cluster. The sudden increase of production at this cluster in December 2014 (Figure 2-2), may have induced this event. In this case the pressure wave would have traveled between 1.4 km and 2.5 km in one month, depending on the reservoir permeability (150 - 500 mD). Again, more observations from induced events are required to support statistical significance to substantiate such a direct relation between seismic events and a sudden increase in production.

2.4 Observed event density from April 2014 to April 2015

Figure 2-3 shows the observed event density for the period from April 1st 2014 to April 1st 2015. The event density was determined using a Kernel Density (standard GIS application) with a radius of 5 km and a cell size of 50 m. As indicated in TNO (2014b), the pressure wave should have traveled approximately 2 to 4 km between January 17th 2014 and April 1st 2014. Therefore April 1st 2014 is chosen as the date after which the rate of seismic events will possibly be affected by the reduction of production.

The average event density is around 0,25 events per km^2 with largest densities in the southwest periphery of the field. Other areas with increased (with respect to the background) event densities during this period are 1) the area west of Delfzijl (Appingedam), 2) the area to the north between Middelstum and Loppersum and 3) the area near Tjuchem (Figure 2-3). Compared to TNO (2014b; Figure 2-5) the areas marked by high event densities correspond well except for the Appingedam area which appears to be characterized by a higher event density now, as shown in Figure 2-3. This means that in the period from November 1st 2014 to April 1st 2015 events have occurred in the Appingedam area. As mentioned previously, the effects of the reduction of production at the nearby Leermens (LRM) cluster to the northwest of Appingedam and the Overschild (OVS) cluster to the southwest of Appingedam seem to be overruled by the ongoing production to the southeast and south of Appingedam (Figure 2-1).

Figure 2-4 shows the event density for the period of April 1st 2014 to April 1st 2015 together with the faults in the reservoir. The match of the event density to two known, mainly NW-SE trending faults systems in the field is striking. One active fault system in the north of the field stretches from the northwest to the east and another active fault system is located in the southwest of the field.

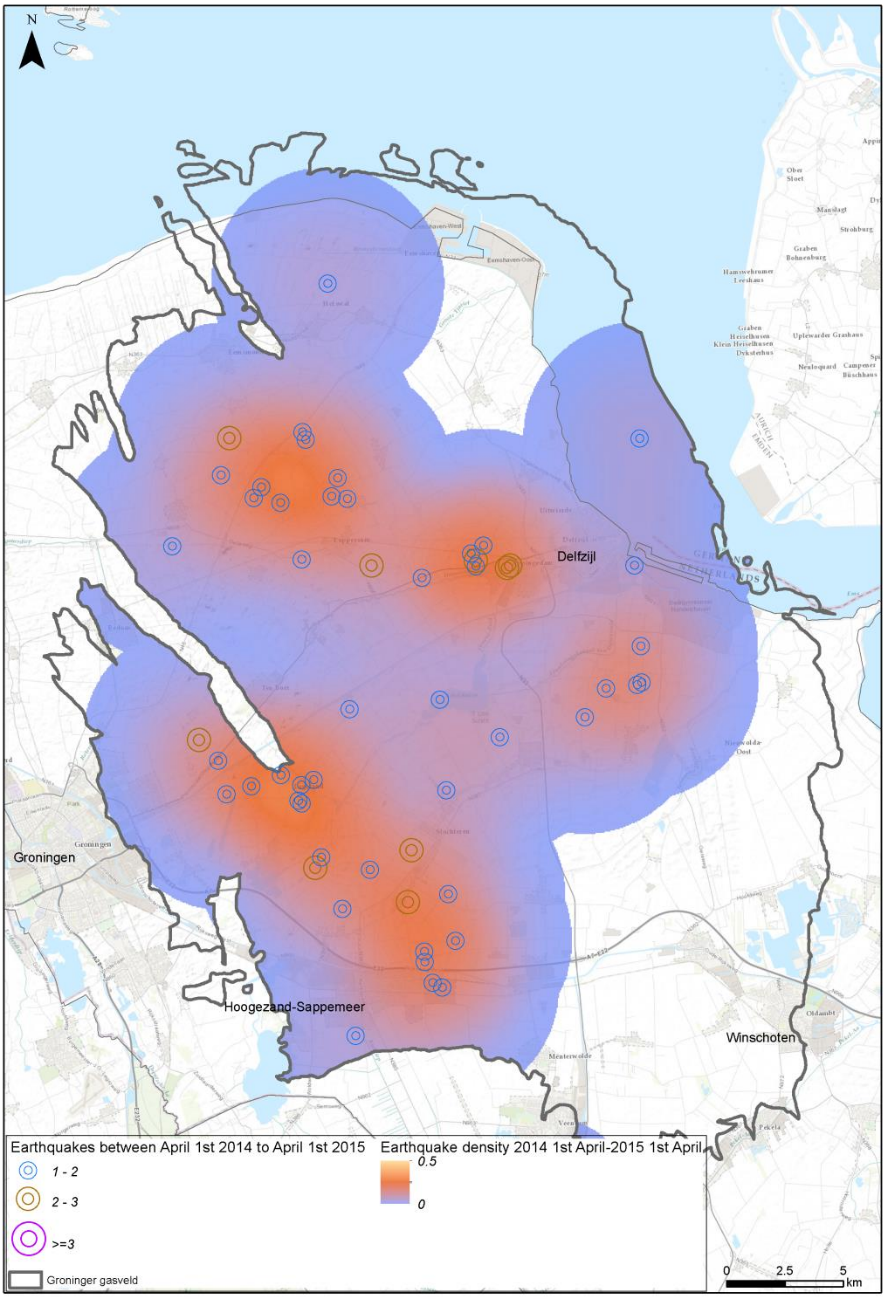


Figure 2-3. Event density (number of events per km^2) from April 1st 2014 to April 1st 2015. The observed events and their magnitudes are indicated by the colored small circles.

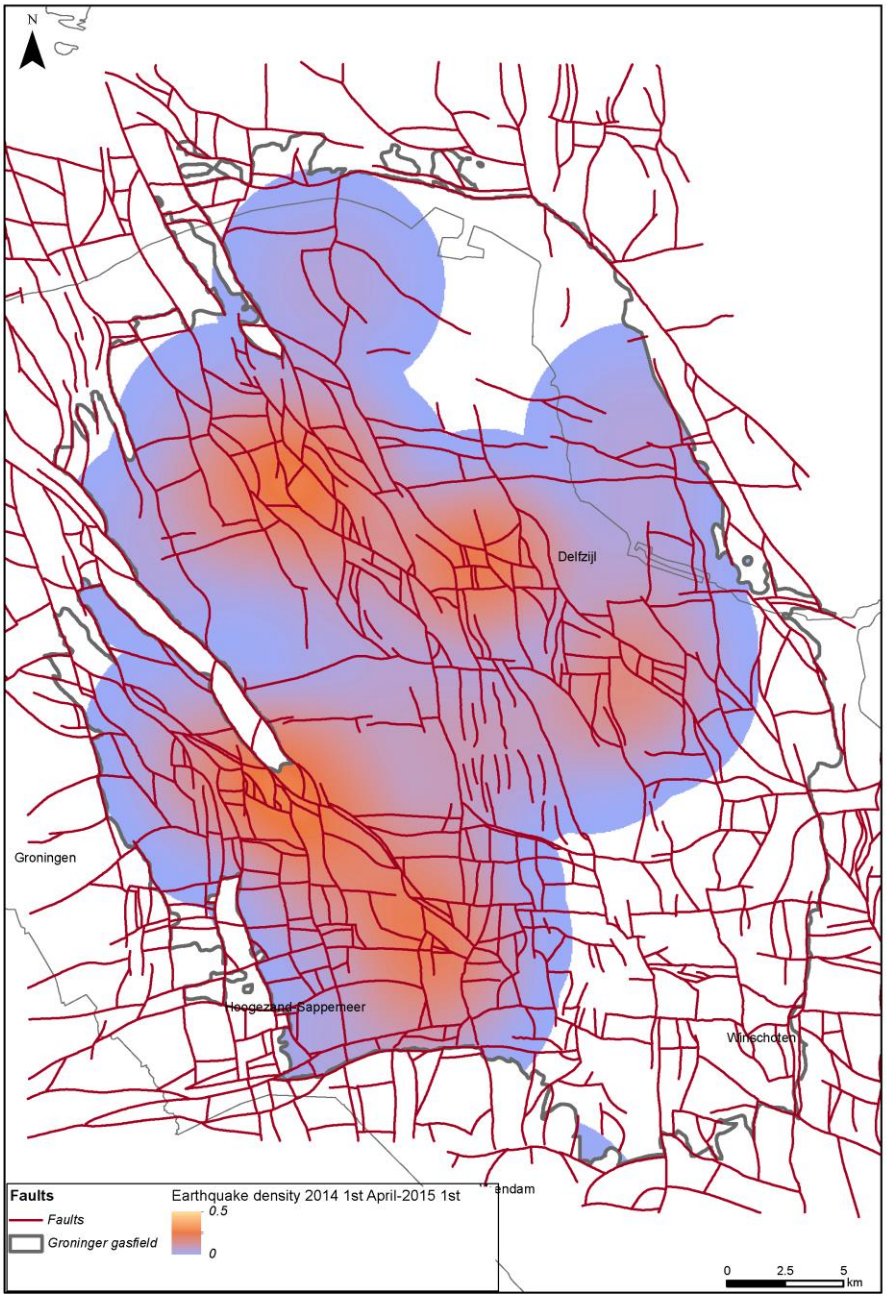


Figure 2-4. Event density (number of events per km^2) from April 1st 2014 to April 1st 2015 shown with the faults in the reservoir (dark red) and the contour of the field (dark blue).

2.5 Comparison to earlier years (2012 and 2013)

In Figure 2-5 and Figure 2-6 the event density is shown for the period April 1st 2012 to April 1st 2013 (Figure 2-5) and April 1st 2013 to April 1st 2014 (Figure 2-6). Compared to Figure 2-3 the amplitudes of the event densities are larger by a factor of 2 (up to 0.5 events per km^2). Also the shape of the event density is different. The largest event densities are observed in the center of the field and in the

Eemskanaal area (Figure 2-1). In Figure 2-7 and Figure 2-8 the difference between the event density in 2014/2015 and the event density in 2013/2014 (Figure 2-7) and the event density in 2012/2013 (Figure 2-8) is shown. In the center a clear decrease in the event density is visible for both difference maps. Thus the event density in the center of the field has diminished since the production reduction of January 2014 compared to previous years.

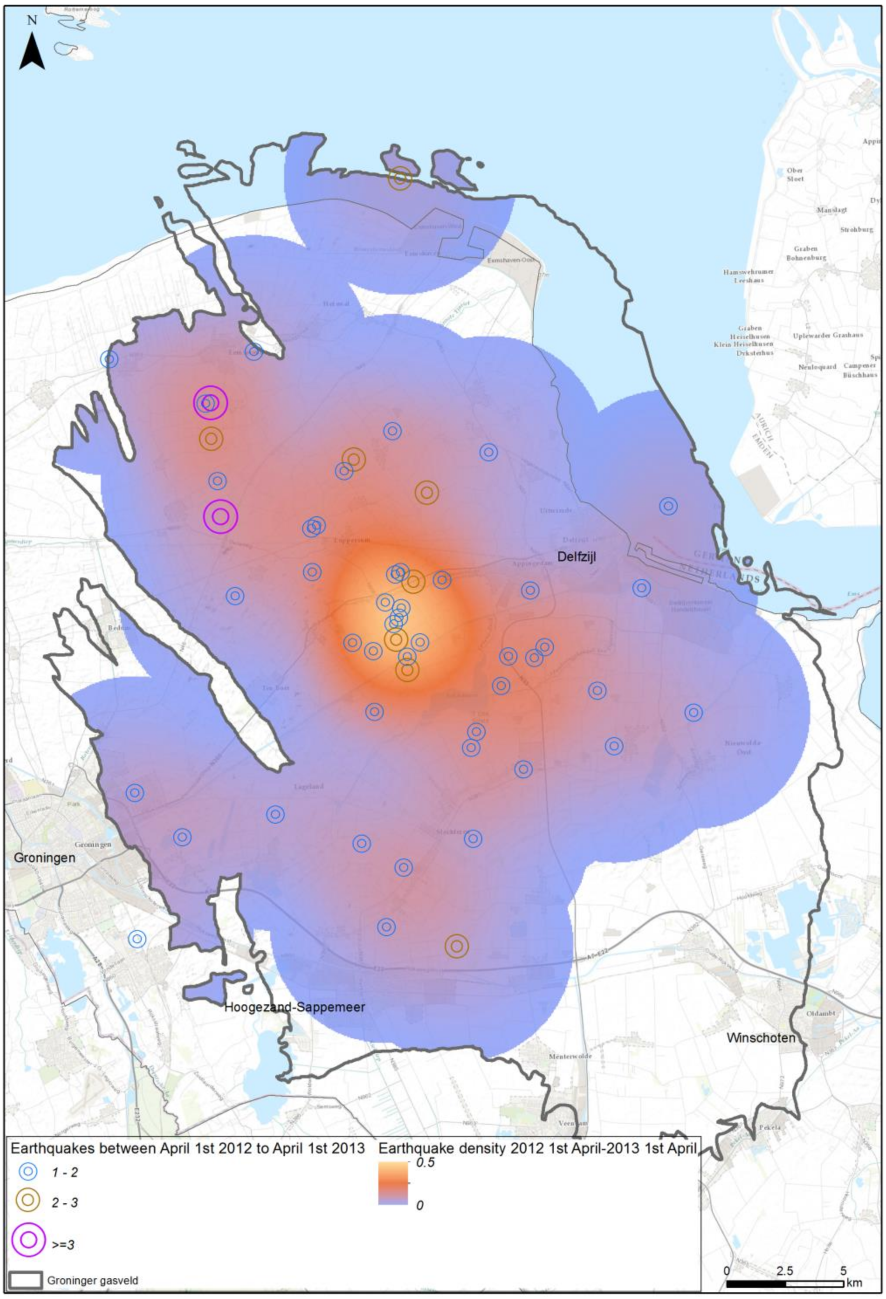


Figure 2-5. Event density (number of events per km^2) from April 1st 2012 to April 1st 2013. The observed events and their magnitudes are indicated by the colored small circles.

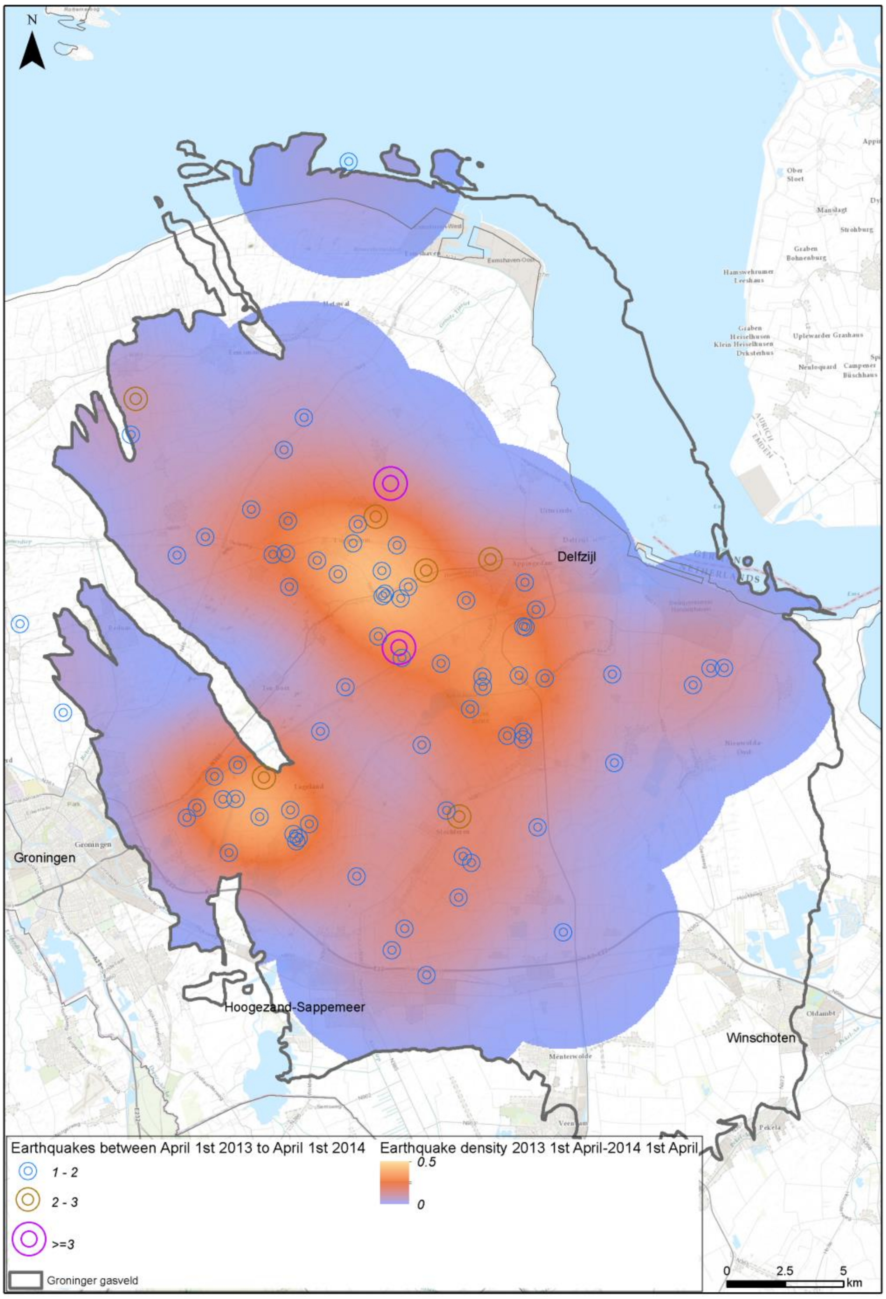


Figure 2-6. Event density (number of events per km^2) from April 1st 2013 to April 1st 2014. The observed events and their magnitudes are indicated by the colored small circles.

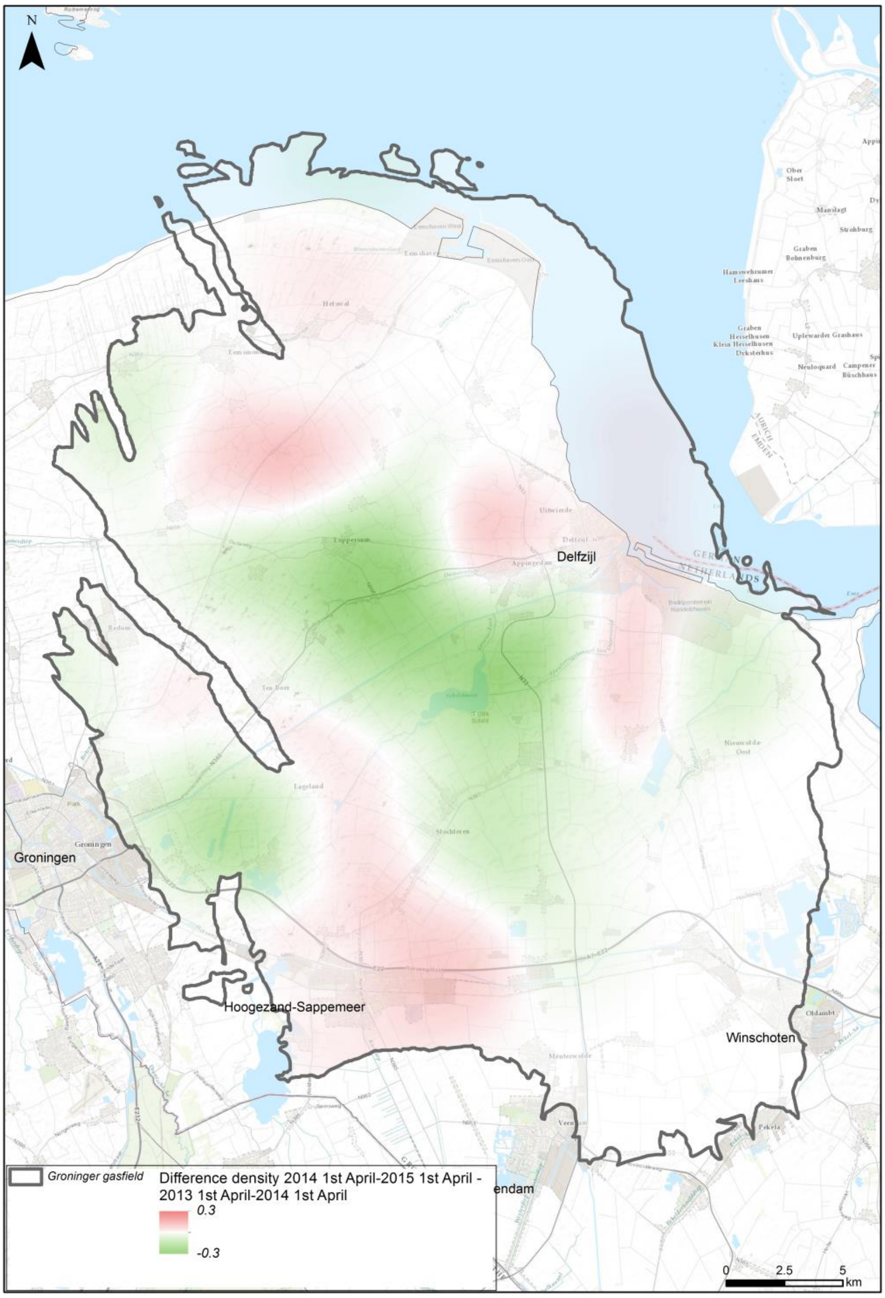


Figure 2-7. Difference in event density (number of events per km^2) between April 1st 2014 - April 1st 2015 (Figure 2-3) and April 1st 2013-April 1st 2014 (Figure 2-6) A negative (green) difference indicates a lower event density in 2014/2015 compared to 2013/2014.

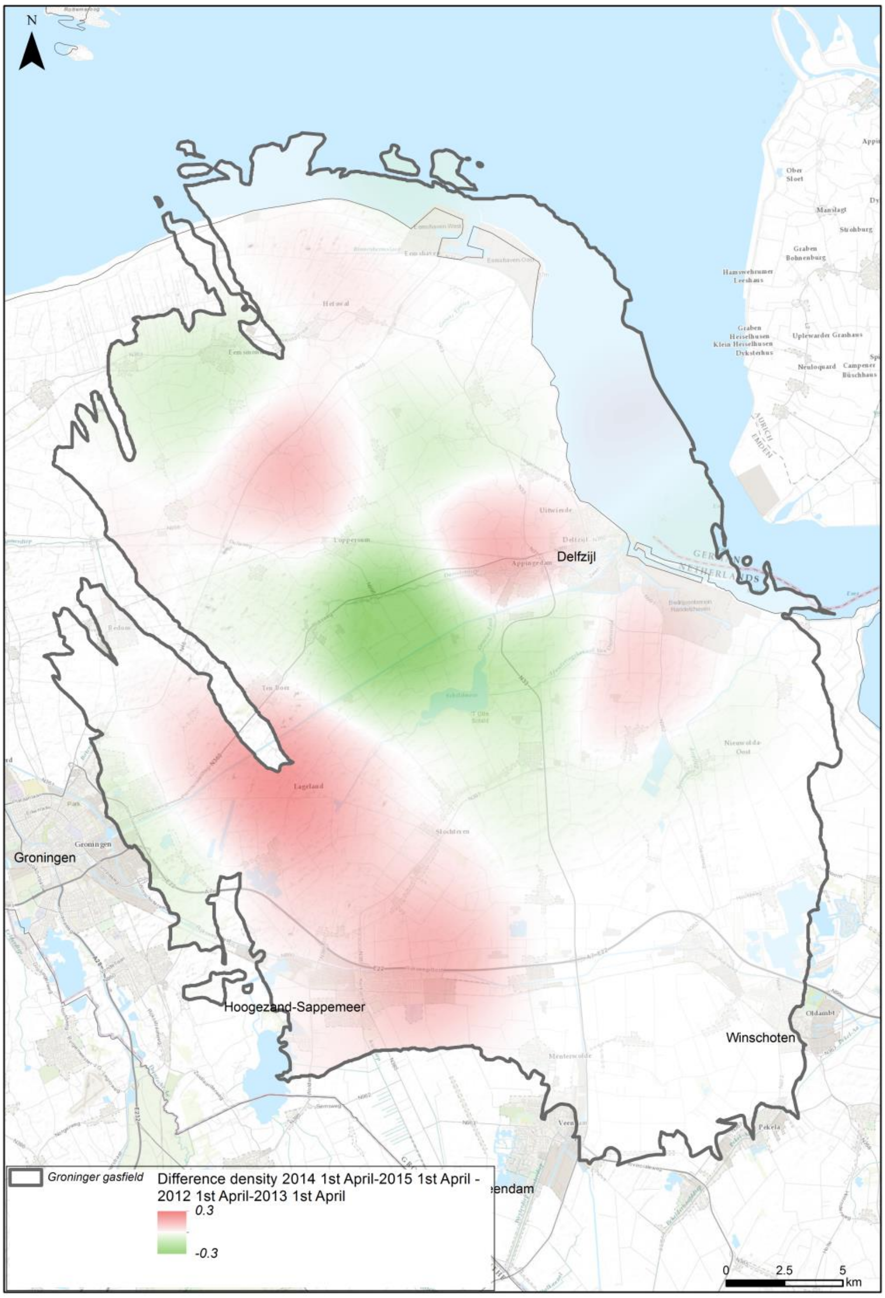


Figure 2-8. Difference in event density (number of events per km^2) between April 1st 2014 - April 1st 2015 (Figure 2-3) and April 1st 2012-April 1st 2013 (Figure 2-5) A negative (green) difference indicates a lower event density in 2014/2015 compared to 2012/2013.

2.6 Statistics of the induced seismicity of the Groningen field

In TNO (2014b) a Bayesian analysis of the event rate from 1991 until November 2014 is presented. Section 2.6.1 provides an update to this analysis. The driver for these statistical analyses was to assess whether a significant change in the

occurrence of events has developed since the production reduction in the center of the field. In this section two different Bayesian methods are shown.

2.6.1 *Previous Bayesian analysis*

The Bayesian analysis in the report of TNO (2014b) assumed three basic trend models: a Poison distribution with a constant, an increasing, and a decreasing seismic event rate. In the period 2003 – January 17th 2014 the rates in three areas of the Groningen field were shown to be increasing. The main question was to investigate whether this trend of increasing events was halted. It was concluded that the chosen method slightly favored a decreasing model, but the data were too sparse to come to a firm conclusion. It turns out that this method will only give a statistically significant answer in 5 to 10 years. Therefore an alternative was used in the next section.

2.6.2 *Alternative Bayesian analysis*

In order to strengthen the results of the previous study we have chosen an alternative approach here. We subdivided the data in segments of 1000 days and looked at a *constant rate model for each segment*. The Poisson model for the rate a is then given as

$$p\,(k \mid a) = (aT)^k \exp(-aT) / k!$$

In each segment we determined the mode of a of the posterior distribution p(a | k), assuming a constant prior p(a). The maximum value of the posterior distribution in each segment is reached for the value a = k / T.

Table 2-3. The number of events in the regions Central, SW and Other as a function of the number of days since the start of observed seismicity on December 5th 1991.

Time (days)	Events $M_L \geq 1$		
	Central	SW	Other
0 – 1000	7	2	20
1000 – 2000	7	0	14
2000 – 3000	12	5	17
3000 – 4000	7	3	11
4000 – 5000	29	7	23
5000 – 6000	31	12	28
6000 – 7000	31	10	49
7000 – 8080	63	19	106
8080 – 8539	11	18	42

The database of the KNMI is used to evaluate the number of events in a given time period and region of the Groningen field. All magnitudes above M_L=1 have been taken into account since the first event on December 5th 1991. The magnitude of completeness (which is the magnitude from which all events over the Groningen field have been registered) changes over the period 1991-2015. The seismometer network was significantly extended up to 1996. The first two time periods (0 - 2000 days) will therefore not have all seismic events included in the database. The magnitude of completeness from 1996 over the whole of the Groningen field is M_L=1.5. We have chosen to take all events from M_L=1, since we analyze different

regions in the field. If the seismometer stations have not changed in this region, all events can be taken into account for a specific region and compared from year to year.

Table 2-4. The event rate, including standard deviation, in the regions Central, SW and Other as a function of the number of days since the start of seismicity on December 5th 1991.

Time (days)	Event rate Central	SW	Other
7000 – 8080	0.058/day ± 0.006/day	0.017/day ± 0.004/day	0.098/day ± 0.01/day
8080 – 8539	0.024/day ± 0.007/day	0.039/day ± 0.09/day	0.091/day ± 0.015/day

Table 2-3 collects the number of seismic events (magnitude $M_L \geq 1$) for each 1000 day period; the corresponding event rate for the 1000 days just before as well as 539 day elapsed since 17 January 2014 are depicted in Table 2-4. The number of events and their event rate is assessed in three regions of the field: “Central” (central Loppersum area), “Southwest (SW)” (line Eemskanaal to the area north of Hoogezand) and “Other” (the remaining part of the field), see TNO (2014b).

These results indicate that:
1) The event rate in the “Central” area has diminished since January 17th 2014.
2) The event rate in the “Southwest” area has gone up by a factor of more than two after January 17th 2014
3) The event rate in the “Other” area has stayed more or less comparable before and after January 17th 2014

There is no doubt that the Central area experienced a significant drop in seismic activity while the southwest area experienced a significant increase in seismic activity. The increase in seismic activity since day 4000 (around 2003) in each of the areas is noteworthy, and this is in line with the increase models used in the previous report (TNO2014b).

2.6.3 Seasonality

In this section the seismic event rate response of the Groningen field is analyzed for correlations with seasonal swings in production.

One way to investigate this is to look at the correlation function between the change in production (*dP*) on a monthly basis and the number of seismic events (*n*) on a monthly basis, *Corr (dP, n)*. Perhaps more tellingly, we may look at the correlation between *dP* and *dn* – the change in seismic events on a monthly basis, *Corr (dP,dn)*. This correlation function is related to the former. The autocorrelation functions of *dP* and *dn* provide additional information.

If we compute the above functions for each year starting in 2003 with a maximum time lag of 36 months the following results ensue:

1) The autocorrelation function for *dP* shows a seasonal trend (Figure 2-10).

2) Since 2005 most years show a positive correlation between production changes and number of monthly events for 2-8 months (Figure 2-11).
3) In all years the correlation between production changes and subsequent *changes* in seismic events is maximum and positive at a lag of some two months (Figure 2-12).

The correlations have been evaluated from 2003 since the seismicity over the field has been more or less constant up to 2003 and increases after 2003 (Figure 2-9).

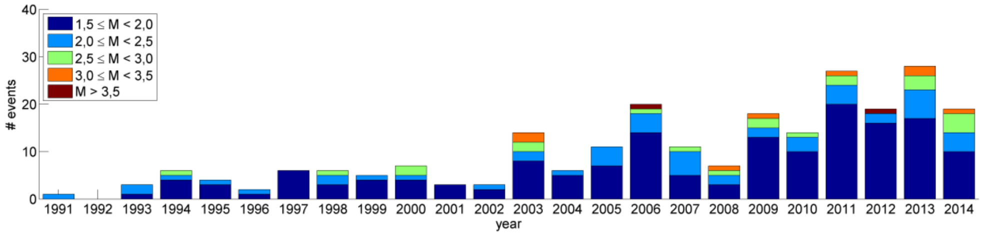


Figure 2-9. Number of events occurring within the contour of the Groningen gas field as a function of time and Magnitude (M).

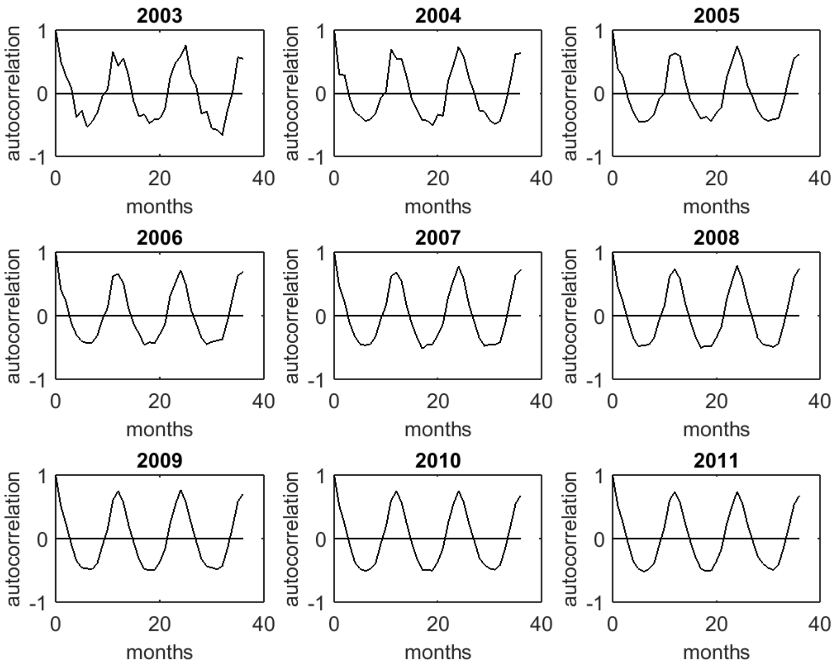


Figure 2-10. Autocorrelation of the production on a monthly basis.

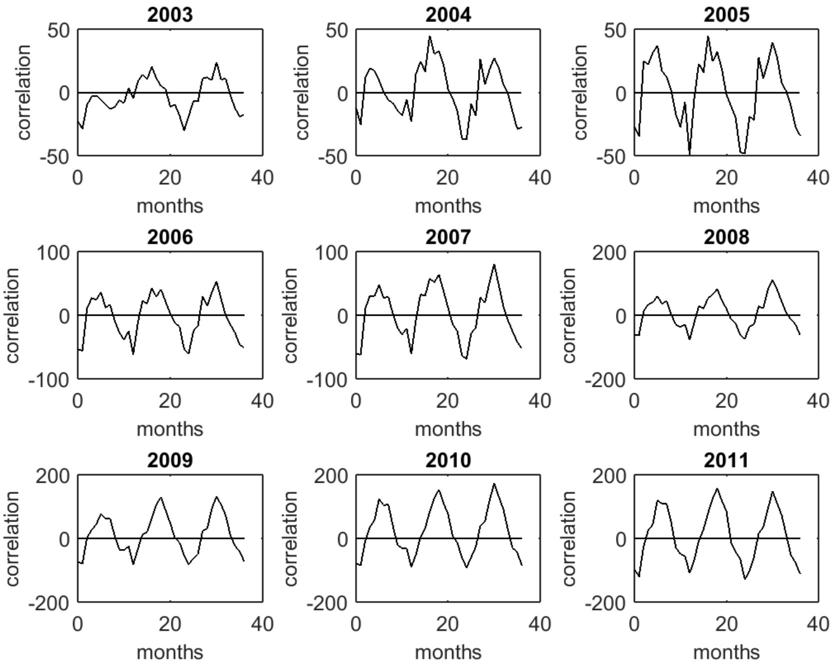


Figure 2-11. The correlation between the production on a monthly basis and the number of seismic events.

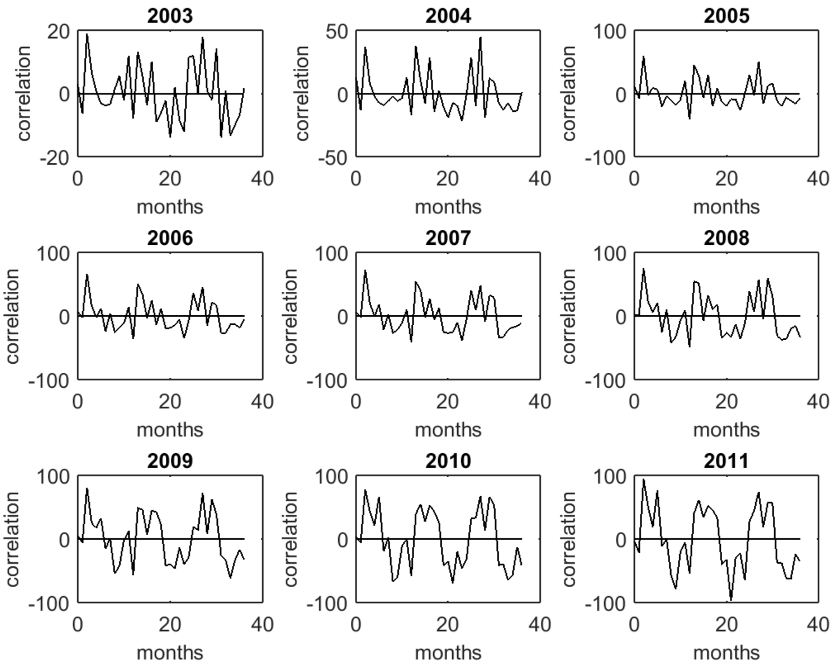


Figure 2-12. The correlation between the production on a monthly basis and the change in seismic events on a monthly basis.

If we compute the (auto) correlation functions over the whole period 2003 to 2014 (maximum lag being 36 months again) we note the following:

1) The autocorrelation function for *dP* shows seasonal effects, as to be expected (Figure 2-13).
2) A yearly pattern is obvious in the correlation between production changes and number of seismic events: After 5-7 months, 17-19 months, and 29-31 months the correlation is maximum positive (Figure 2-14).
3) The two-months effect in 3) is still present, but it is no longer predominant. Stacking of all data apparently washes this effect away (Figure 2-14).

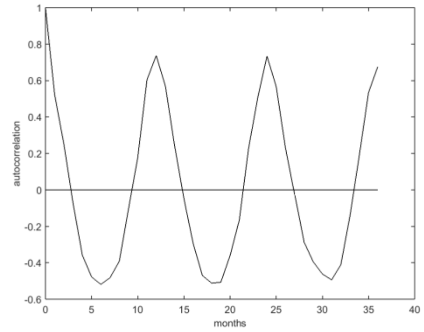


Figure 2-13. Autocorrelation of the production on a monthly basis.

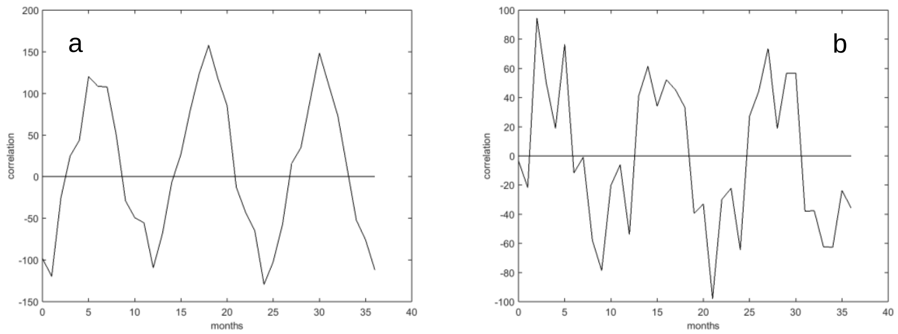


Figure 2-14a.) The correlation between the production on a monthly basis and the number of seismic events and b.) The correlation between the production on a monthly basis and the change in seismic events on a monthly basis.

All together we infer seasonal effects in the seismicity. Since the production changes follow more or less identical patterns each year it is not possible to attribute the values of the correlation functions at year Y exclusively to the production changes in *that* year. It is well worth remembering that correlation does not prove a causal relation. However, what we see is seasonality, whatever the precise mechanical processes in the subsurface.

2.7 Bayesian point change model

2.7.1 Introduction

Change point models are used to detect changes in occurrence rates of events. Gupta and Baker (2015) have developed a Bayesian Point Change model which quantifies the changes in seismicity rates for Oklahoma US. The unknown parameters in this model are the date of change, the event rate before the change and the event rate after the change. In Oklahoma a marked increase in seismicity was observed after 2008 (Gupta and Baker 2015) and it was confirmed that the change point occurs around 2008-2010. Furthermore the post change date seismicity rate is 300 times the pre change date seismicity rate, indicating a significant increase in the number of seismic events.

2.7.2 Results of Bayesian Change Point Model for $M_L \geq 1.5$ and 1991-2015

In this section the Bayesian Point Change Model (Appendix B) is applied to the observed seismic events of the Groningen field. From the seismicity database of the KNMI (www.knmi.nl), only the events with magnitudes larger than M_L=1.5 that occur within the contours of the Groningen gas field were selected. The magnitude M_L of 1.5 (magnitude of completeness) is chosen as it represents the events which can be recorded over the entire field since January 1996. For the analysis a point in the center of the field (latitude=53.23 and longitude =6.716) and a radius of 50 km is defined, such that all induced events related to the Groningen gas field are selected for the analysis.

Figure 2-15 shows the results of the Bayesian Point Change analysis; a change point is observed for January 12th 2003. In Figure 2-16 the pre change date and post change date event rates are shown. The pre change event rate is around 0.01 events per day, corresponding to 3-5 events per year. The post change event rate approximates 0.05 events per day, corresponding to 15-20 events per year. This corresponds quite well to the observed seismic events (Figure 2-9).

After 2009 no change point is observed for all events with magnitudes larger than M_L=1.5. The analysis cannot provide a change point for the period after January 2014 when production was changed over the field due to the relatively small number of events after January 2014.

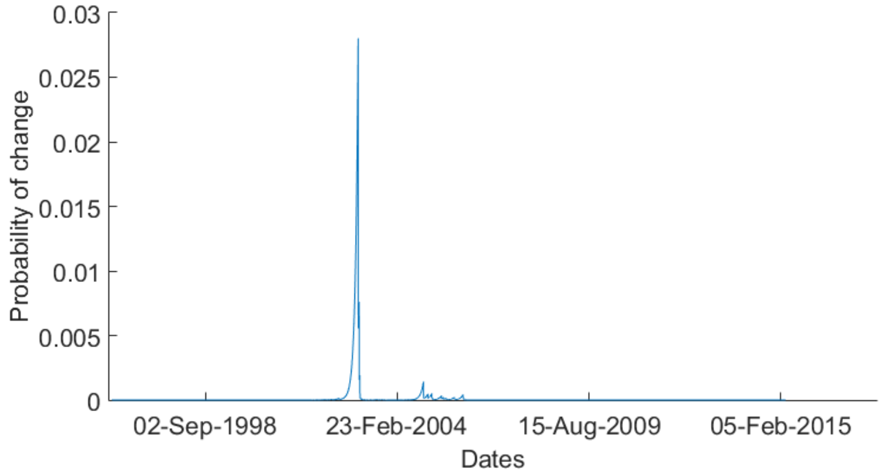


Figure 2-15. The probability of change in time over the period of 1991 up to now.

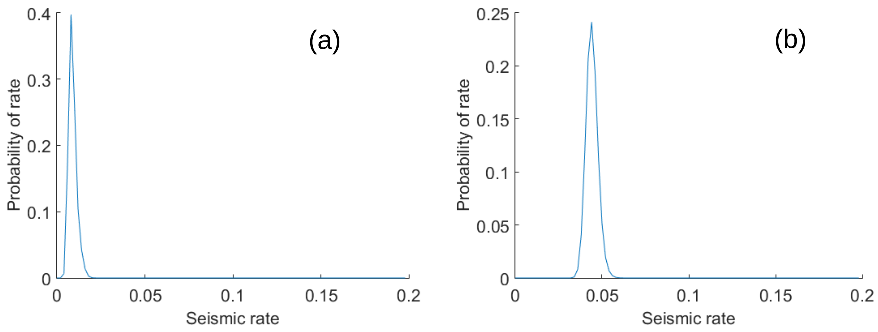


Figure 2-16a.) The pre change date event rate (in events/day) and b.) the post change date event rate (in events/day)

2.7.3 Results of Bayesian Change Point Model for various locations over Groningen field

For this analysis an array of points located at approximately 5 km from each other, distributed regularly over the Groningen field is investigated. For each location a radius of 10 km around the investigated point is taken into consideration. In this way the Groningen field is divided in 50 overlapping regions. The probability of change in event rate is calculated for each local region and for all events with magnitudes larger than M_L=1.5 over the period from 1991 to now. The result is presented in Figure 2-17.

The Bayesian change point model has detected when event rates have changed over the entire Groningen field. The earliest change of event rate happens in the central part of the field (January 2003). In time the event rate changes spread towards the edges of the field. This corresponds to earlier observations of the spread of events in time (e.g. NAM 2013). At the south and north edges no change of event rate could be detected due to the few recorded events in the 10 km radius from the investigated points.

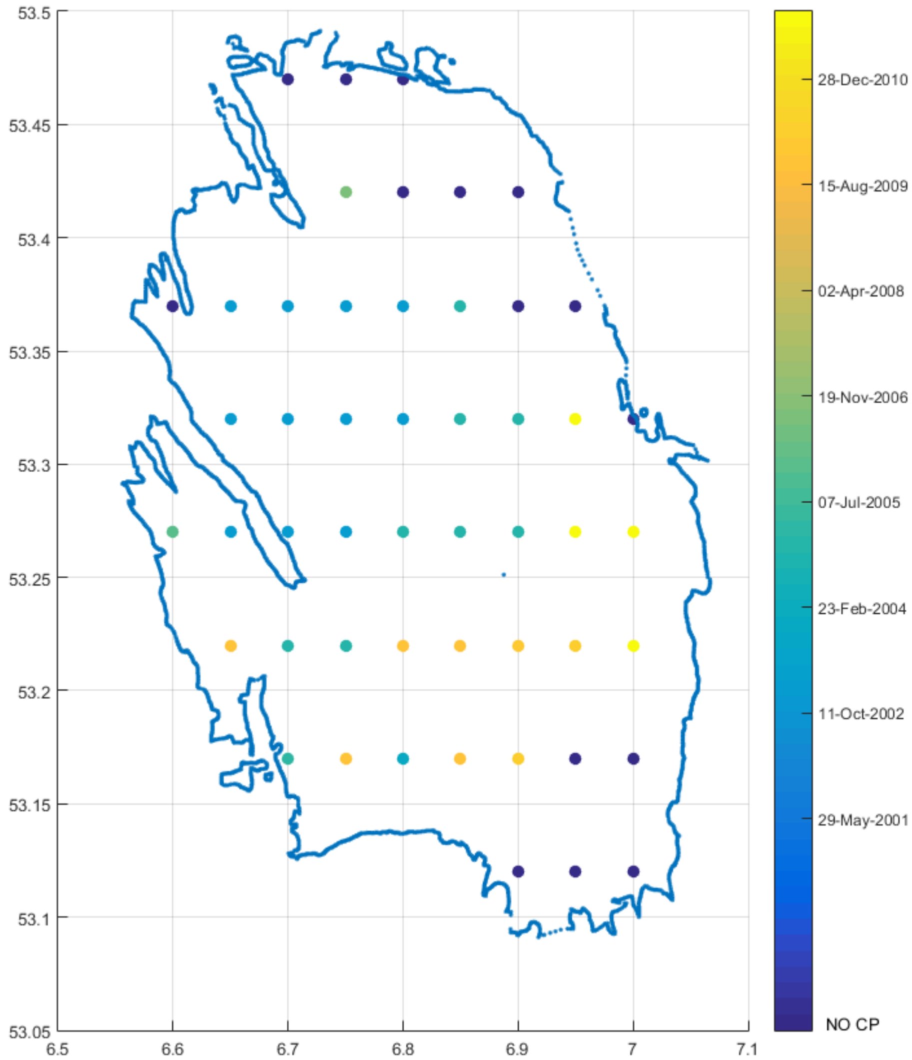


Figure 2-17. Time of event rate changes evaluated at 50 local points in the Groningen field.

3 Compaction field up to 2013 from Inversion

3.1 Introduction

In TNO (2013) and TNO (2014b) possible inconsistencies were identified in the geological model of the field, mainly by the mismatch between the modeled subsidence and the measured subsidence. In these reports we have used the so-called forward method, illustrated by Figure 3-1. In the forward model gas production is used to model the reduction of pressures in the field. The reduction of pressure gives compaction in the field, using a compaction model. Using a transfer function compaction can be translated to subsidence at the surface (e.g. Van Opstal 1974). This forward procedure is sensitive to the quality of the geological model and the reservoir dynamical model. As is described in TNO (2013, 2014b), mismatches between modeled and measured subsidence were identified leading to possible inconsistencies in the porosity and aquifer activity.

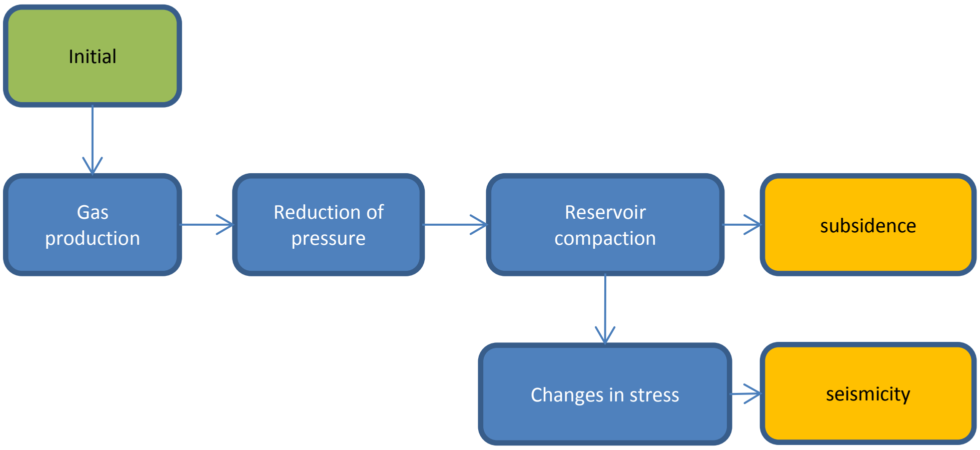


Figure 3-1. Schematics of the forward method.

The opposite of the forward method is given by the inverse method. In this method the measured subsidence is used to compute compaction. The inverse method is sensitive to the quality of the subsidence measurements but not sensitive to the quality of the geological and the reservoir dynamical model. The identified problems in the geological and reservoir dynamical model have led to the implementation of the inverse method, described in section 3.2, to provide an alternative compaction field for Groningen.

3.2 The inverse model & double differences

As the inverse method is sensitive to the quality of the subsidence measurements the double differences measured between optical levelling points have been used. Therefore problems with reference points have been avoided. The inverse method is described in detail in appendix A in the form of a conference paper submitted on May 1st 2015 to NISOLS (*Ninth International Symposium on Land Subsidence*).

In this study the compaction field from TNO (2014b) has been used as input to the inversion. This ensures a new corrected compaction field with similar spatial resolution as the previous compaction field. In the inversion procedure correction factors to the previous compaction field have been sought. These correction factors are applied to the prior compaction field to arrive at the estimated compaction field. Figure 3-2 shows the prior compaction field and the estimated compaction field in 1993 and 2013.

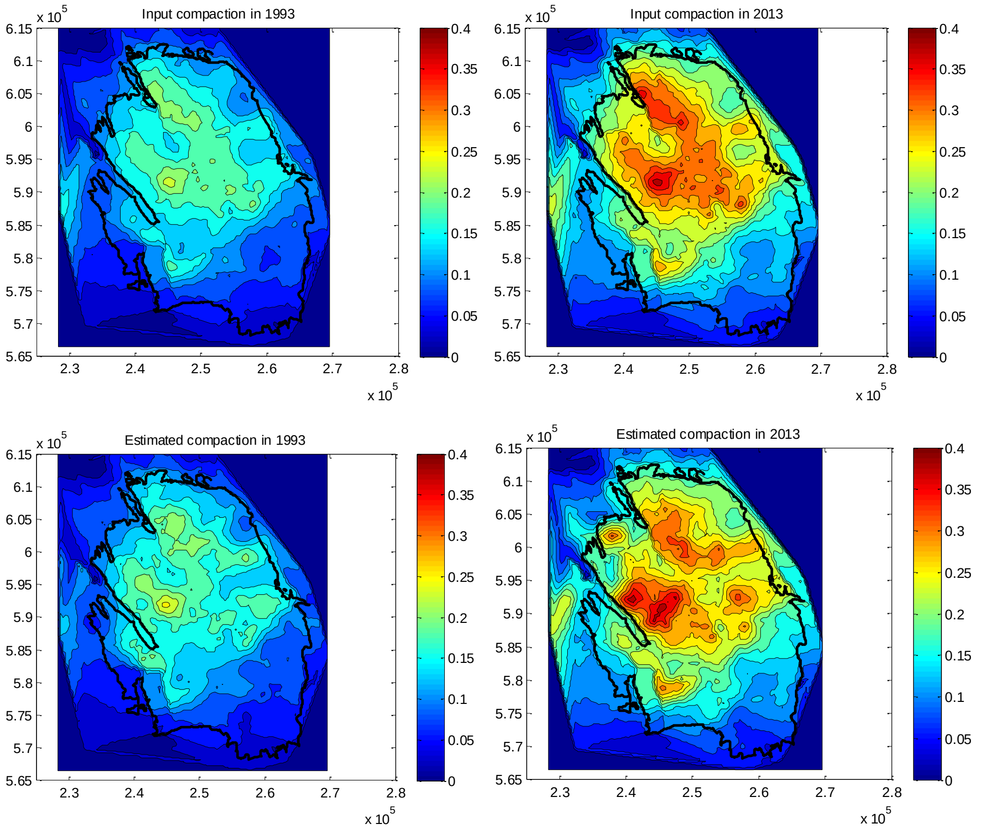


Figure 3-2 Prior compaction fields (top row) and estimated compaction fields (bottom row) in 1993 (left) and in 2013 (right)

Figure 3-3 shows the compaction field in 2013 derived from the inversion of subsidence data together with the faults in the geological model (NAM, 2013). Compaction differs from the prior model, described in TNO (2013, 2014a, 2014b). There are four areas (Figure 3-2, bottom right) showing higher compaction (>30 cm) of which one is located in the northeast, one in the middle, one in the east (close to Appingedam) and one in the south (north of Hoogezand) of the field. Compared to TNO (2013, 2014a, b) the area of maximum compaction has shifted to the west. Areas characterized by high compaction also seem constrained by faults systems, which leads to enhanced differential compaction across faults (Figure 3-3).

Figure 3-4 shows the same compaction results from inversion in 2013, but now including the locations of observed seismic events. The seismic events are concentrated in a band from Northwest to Southeast. Contrary to earlier results, the areas with high seismic event densities do not correlate with areas of high compaction; they correlate with a concentration of faults. This indicates that the

faults play a major role in the distribution of seismicity. There seems to be no correlation with the offset of the faults (Figure 3-5). Finally Figure 3-6 shows the difference in compaction between the model of TNO (2014a) and the resulting compaction field derived through inversion. The areas with the largest differences correspond to the areas where subsidence was poorly matched (Figure 3-7). These areas correspond to areas where TNO has discussed NAM's porosity estimations or areas where active aquifers are assumed in the subsurface model, as has been described in TNO (2013, 2014b).

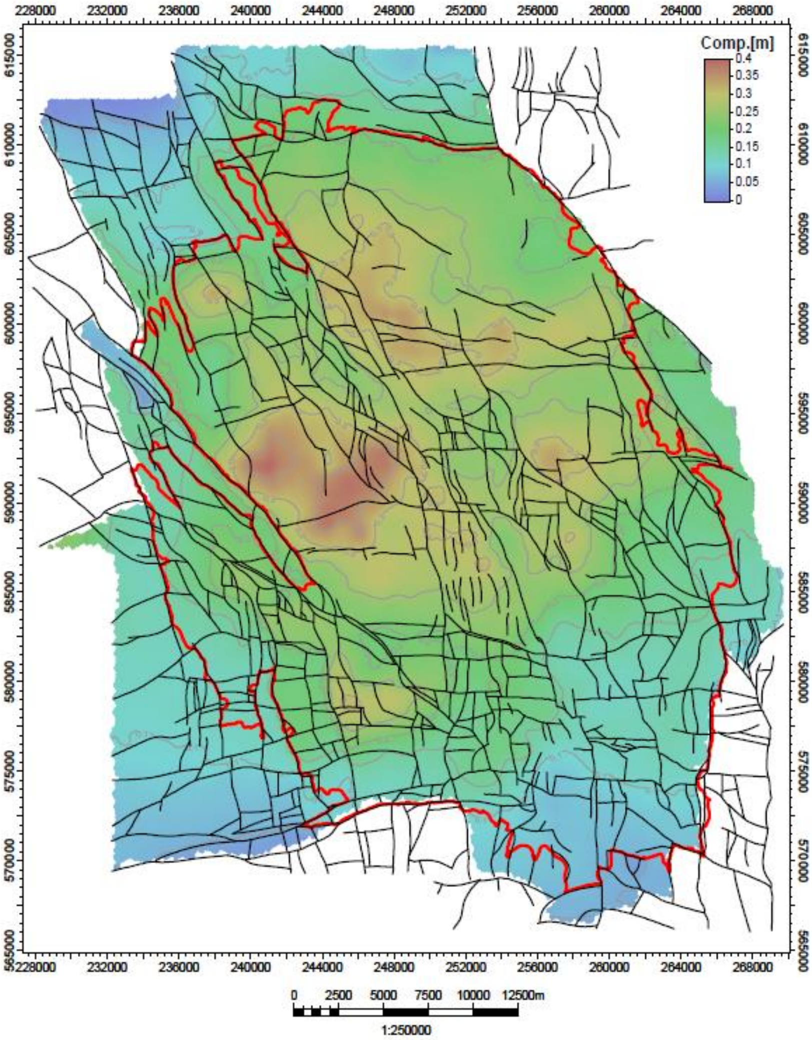


Figure 3-3. Compaction (m) in 2013 obtained through inversion of subsidence measurements (section 3.1). The red line gives the contour of the Groningen field and the black lines are the faults that are present in the geological model in Petrel (NAM, 2013).

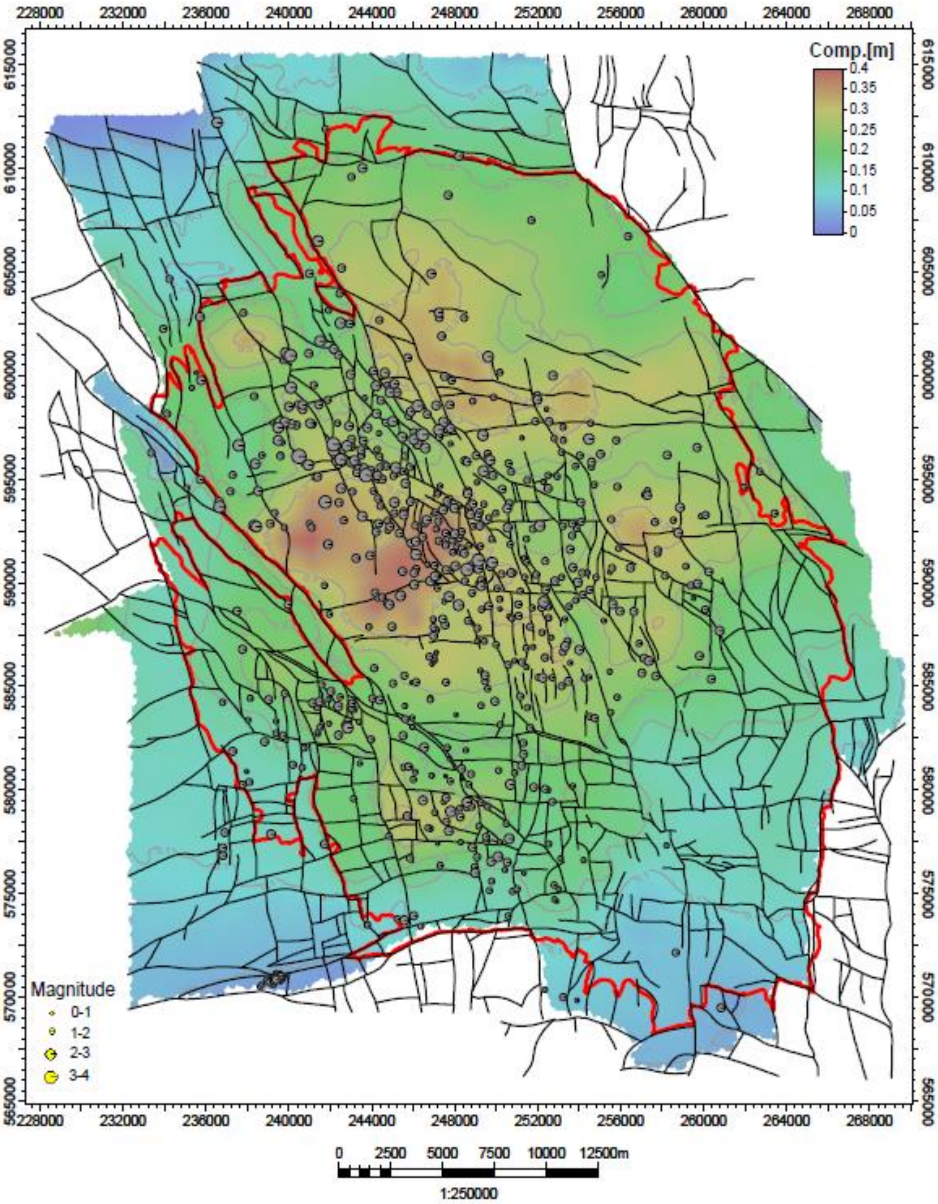


Figure 3-4. Compaction (m) in 2013 obtained through inversion of subsidence measurements (section 3.1). The red line gives the contour of the Groningen field and the black lines are the faults that are present in the geological model in Petrel (NAM, 2013). Also shown is the seismicity in the field, the size of the symbols indicates the magnitudes of the events.

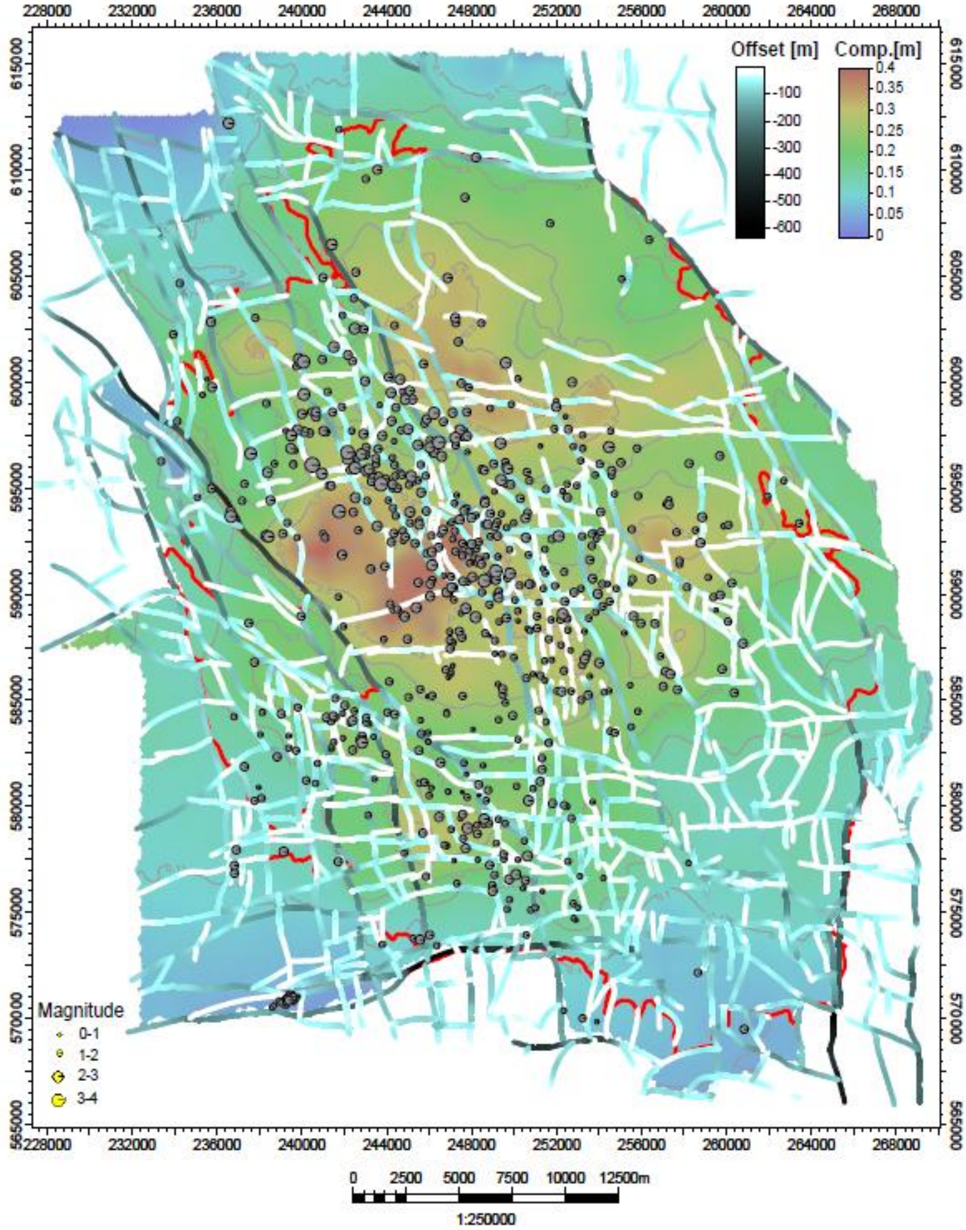


Figure 3-5. Compaction (m) in 2013 obtained through inversion of subsidence measurements (section 3.1). The red line gives the contour of the Groningen field and the faults in the geological Petrel model (NAM, 2013) are indicated with their offset.

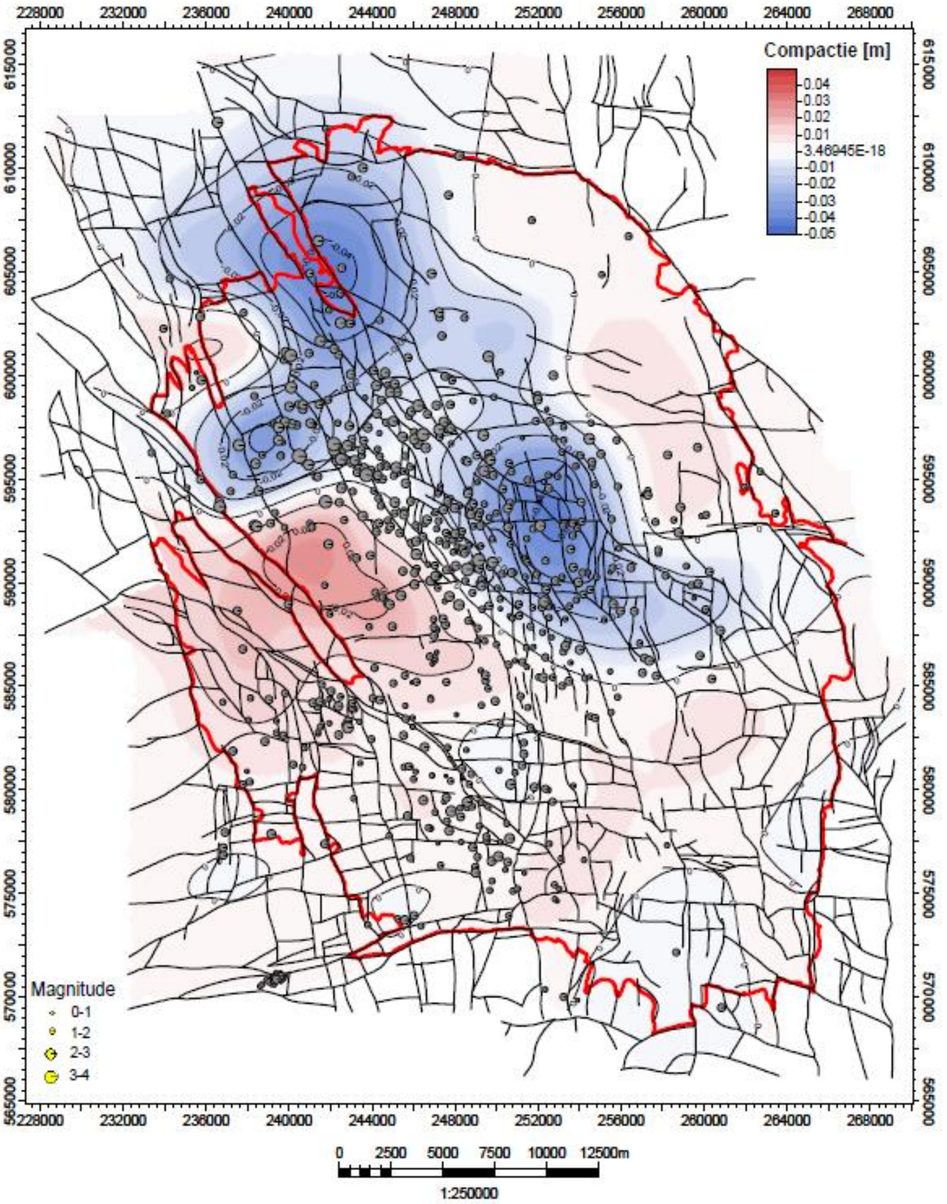


Figure 3-6. The difference between the compaction field of TNO (2013, 2014a,b) and the compaction field resulting from inversion (m).

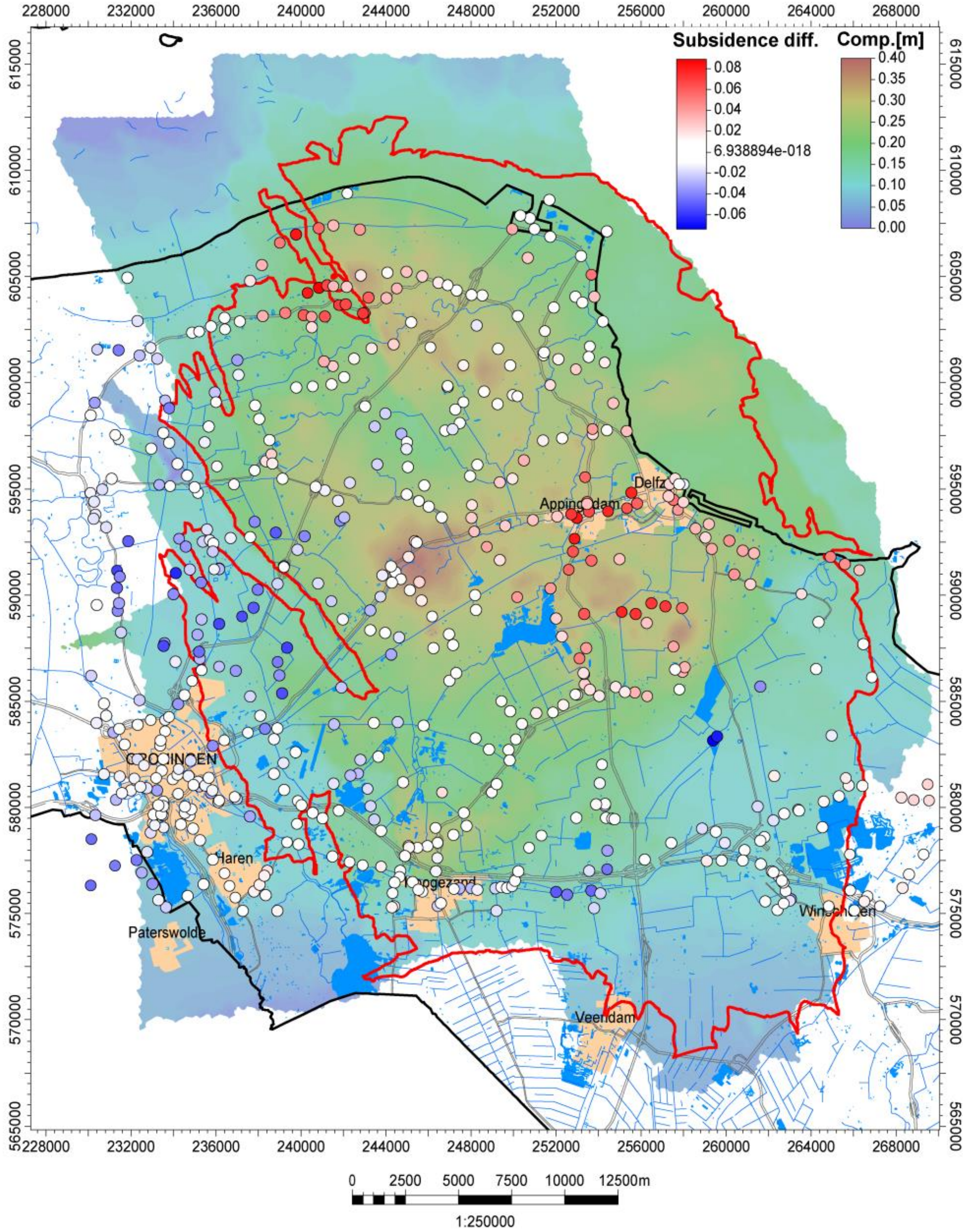


Figure 3-7. Figure 5.13 from TNO (2013). Compaction in 2012 calculated with the RTiCM model using the subsurface model.

4 Main Findings

In 2014 the total gas production of the Groningen gas field was 42,41 bcm, which is less than the imposed production cap of 42,5 bcm. The Loppersum production clusters (LRM, PAU, POS, OVS and ZND) produced in total 2,57 bcm in 2014, which is below the production cap of 3 bcm. Production varied over the year with the majority of gas being produced during the winter months.

In support of their advice, State Supervision of Mines has requested the following additional technical evaluations from TNO-AGE:

- An update on the seismicity of the Groningen field
- compaction field based on inversion of subsidence data

Update on the seismicity of the Groningen field

The distribution of higher magnitude (M_L>2) events occurring since September 2014 can be explained by

- The distances to producing clusters vs non-producing clusters which can explain the events close to Appingedam
- The increase of production at the Ten Post cluster (POS) in December 2014

The first explanation would indicate that the effect of reducing production of the Loppersum clusters has been partially overruled by production of other clusters close to Appingedam. The second explanation would indicate that sudden increases in production could lead to a changing pattern of events in time and space. The latter statement cannot yet be proven with statistical significance and should therefore be further evaluated. An analysis of production and seismic events occurring over time could possibly provide further statistical significance.

The observed density of seismic events from April 2014 to April 2015 is different from densities observed during earlier years. Largest seismic event densities are concentrated in the southwest while the center of the field is marked by lower densities. In previous years the density of seismic events in the center were highest in the Groningen field (see also TNO 2014b). This indicates that the reduction of production in the central area has a marked influence on the number of events in the same area. Additionally, there is a striking match of the event density in 2014/2015 to two known fault systems in the field. These fault systems correspond to areas in the field where differential compaction, known to be an indicator for the occurrence of seismic events, exists (Figure ii).

Statistical analysis on the number of seismic events indicates that the number of events per day in the center of the field has halved since January 2014. The southwestern area, however, shows an increase in the number of events per day. Similar to the production, the seismic events of the Groningen fields exhibits clear seasonality with a lag of some two months between production changes and a change in seismic events.

A Bayesian change point model that has been successfully applied in Oklahoma, U.S.A., has also been applied to the Groningen gas field. A change point in the center of the field is found in January 2003. Event rates after 2003 have quadrupled

compared to the years prior to 2003. This would indicate that the fault system in the center of the Groningen field has reached criticality in the beginning of 2003, i.e. small changes in stress will lead to seismic events. Over the whole of the field change points are identified which vary in time (from 2003 to 2010); the earliest times in the center of the field and later times at the edges of the field. This corresponds to the observation that events have started to occur in the center of the field and have spread in time over the field. If the change point indicates when a fault system becomes critical then this also means that different fault systems have become critical at different times.

After 2009 no change point in the center of the field has been found for seismic events with magnitudes larger than M_L=1.5. The number of events (ML≥1.5) since 2014 is probably not enough to show a change point in event rates. Thus this data cannot be used to prove statistically significant changes in event rates since the production reduction of January 2014.

Alternative compaction field

Inversion of subsidence data has provided a correction to the compaction field presented in TNO (2013, 2014a,b). The correction is predominantly applied in regions where previously erroneous porosity estimations or aquifer activity were suspected. The area of maximum compaction has shifted to the west and does not correspond to the area of maximum event density in the center of the field. This indicates that in this regard the presence of faults is more important for seismicity than the compaction itself. Also differential compaction, known to be an indicator for the occurrence of seismicity, is visible over faults.

This leads to the conclusion that the existing seismological model which NAM has used in the production plan (NAM, 2013), based on an empirical relation between total compaction and the occurrence of events, needs to be updated. As indicated in TNO (2013, 2014a,b) the faults in the reservoir play an important role in the occurrence of events within the field and therefore they have to be taken into account in any future seismological model.

5 References

EZ 2014 Brief van de Minister van Economische Zaken aan de Vaste Kamercommissie (kenmerk: DGETM/ 14008697), 17 januari 2014

Gupta and Baker 2015 A. Gupta, and J. Baker, A Bayesian change point model to detect changes in event occurrence rates, with application to induced seismicity, *12th international Conference on Applications of Statistics and Probability* in Civil Engineering ICASP12, Vancouver, Canada, July 12-15, 2015.

NAM 2013 Wijziging winningsplan Groningen 2013, inclusief technische bijlage Groningen winningsplan 2013. Versie 29 november 2013.

NAM 2014 Hazard Assessment for the Eemskanaal area of the Groningen field. Versie 15 november 2014.

NAM 2014 b Addendum to Hazard Assessment for the Eemskanaal area of the Groningen field.

Pruiksma et al 2014 J. P. Pruiksma, J.N. Breunese, K. van Thienen-Visser, J.A. de Waal. Isotach formulation of the Rate Type Compaction Model for Sandstone, *submitted to International Journal of Rock Mechanics and Mining Sciences*, October 2014.

Roest and Kuilman 1994 J.P.A. Roest and W. Kuilman, Geomechanical analysis of small earthquakes at the Eleveld gas reservoir. Rock mechanics in Petroleum Engineering, 29-31, August 1994.

TNO 2013 Toetsing van de bodemdalingsprognoses en seismische hazard ten gevolge van gaswinning van het Groningen veld. TNO rapport 2013 R11953, 23 december 2013.

TNO 2014a Technisch rapport behorende bij “Effecten verschillende productiescenario’s op de verdeling van de compactie in het Groningen veld in de periode 2014 t/m 2016”. TNO rapport 2014 R10426, 7 maart 2014.

TNO 2014b Recent developments of the Groningen field in 2014 and, specifically, the southwest periphery of the field. TNO rapport 2014 R 11703, 9 December 2014.

Van Opstal 1974 G. van Opstal, The effect of base rock rigidity on subsidence due to compaction, Proceedings of the Third Congress of the International Society of Rock Mechanics,

Denver, Colorado, September 1-7, 1974. Volume II, part B, National Academy of Sciences, Washington, D.C. 1974.

6 Signature

Utrecht, 29 May 2015 TNO



Dr. I. C. Kroon	Karin van Thienen-Visser, Peter Fokker, Manuel Nepveu, Danijela Sijacic, Jenny Hettelaar, Bart van Kempen
Head of department	Author

A Inversion of double-difference measurements from optical levelling for the Groningen gas field

This appendix has been submitted as conference paper on May 1st to NISOLS (Ninth International Symposium on Land Subsidence). This conference paper will be reviewed by external experts and after revision and resubmitting it will be presented on NISOLS, Japan, November 2015.

Peter A. Fokker and Karin Van Thienen-Visser
TNO, Utrecht, The Netherlands
Correspondence to: Peter A. Fokker (peter.fokker@tno.nl)

Abstract
Hydrocarbon extraction lead to compaction of the gas reservoir which is visible as subsidence on the surface. Subsidence measurements can therefore be used to better estimate reservoir parameters. Total subsidence is derived from the result of the measurement of height differences between optical benchmarks. The procedure from optical height difference measurements to absolute subsidence is an inversion, and the result is often used as an input for consequent inversions on the reservoir. We have used the difference measurements directly to invert for compaction of the Groningen gas reservoir in the Netherlands. We have used a linear inversion exercise to update an already existing reservoir compaction model of the field. This procedure yielded areas of increased and decreased levels of compaction compared to the existing compaction model in agreement with observed discrepancies in porosity and aquifer activity.

Introduction
The Groningen gas field is a giant onshore field that has caused substantial subsidence since the start of its production in 1963. This subsidence has periodically been established by measuring the difference in height of stable benchmarks, using optical levelling. Pressures in the field have been closely monitored for reservoir management. History matching of the reservoir model on the observed pressures has resulted in a reasonably accurate pressure distribution development over the field.
There are a number of parameters in the relationship between the reservoir pressure and the subsidence which are more or less uncertain. The first one is the compaction coefficient, being dependent on the rock type and the porosity. There is also some uncertainty in the pressure estimates in some regions of the field, particularly in the connected aquifers, where pressure measurements are not available.
In the present paper we use the raw leveling difference measurements in conjunction with the prior knowledge about the Groningen gas reservoir in order to constrain the uncertainties. We employ an inverse algorithm to this end, but, instead of using interpreted heights, we use the originally measured height differences. In an earlier paper we reported the benefits this approach [Fokker and Van Thienen-Visser, 2015].

Available data

The Groningen gas field has been in production since 1963. It is located onshore in the Northeast of the Netherlands. Extensive geological, geophysical and reservoir engineering data have been used to history-match the reservoir characteristics like geometry, porosity and permeability. We had access to the simulated pressure field at yearly dates from 1/1/1964 to 1/1/2017. The delta pressures were multiplied by the height and the estimated compaction coefficient for each grid cell, based on lithology, pressure depletion and porosity. For each x-y location these numbers were accumulated over the reservoir layers in order to yield a prior estimate for the compaction grid at 9070 x-y locations for 54 times [Van Thienen-Visser et al., 2015]. We remapped the provided compaction values to locations on a regular 400x400 m^2 grid for later manipulation. A map of the input compaction grid and the outline of the Groningen gas field in 2012 is provided in Fig. 1.

In the present study we focused on the use of data acquired through optical levelling. Usually, investigators use differences of the interpolated height maps to estimate surface movement. The procedure to obtain these differences includes the coupling to a reference benchmark or a set of reference benchmarks which are supposed to be stable, by integrating along the path of measurements to the stable benchmark. This procedure is sensitive to errors in the network and it accumulates the inaccuracy of all the measurements in the connecting path. The latter drawback can be addressed by providing the full covariance matrix of the resulting height estimates; this is, however, rarely done. Also reference benchmarks which, in hindsight, are not stable give rise to further inaccuracies. We have therefore chosen to use height difference measurements directly. The procedure to obtain double-difference estimates has been outlined in an earlier paper [Fokker and Van Thienen-Visser, 2015]; it involves the determination of height differences between corresponding benchmark pairs in subsequent measurement campaigns, which have not necessarily been achieved in the same order.

Optical levelling campaigns have been performed many times in Groningen with different coverage. We had access to a total of 92 campaigns, dating from 1938 to 2012. Within a total of 7995 benchmarks, more than 26,000 height differences had been measured. In this set, 1572 benchmarks had been identified as stable ones in the resulting optical levelling database. We have constructed differences between stable benchmarks only, using the measurement paths along the unstable ones, and used these to construct the double differences. Further, we discarded benchmarks west of the line with x = 230,000 m and south of the line with y = 575,000 m in the local coordinate system (RD) to exclude the influence of other sources of compaction in those areas (e.g. the depletion of the Annerveen gas field south of Groningen). Still, a total of 10860 double differences could be constructed between 987 benchmarks. The locations of these benchmarks are shown in Figure 1.

Forward model

Gas production causes reservoir compaction, which, in turn, results in surface movement. Compaction in the reservoir may also change certain reservoir parameters. For the current study, a one-way coupling suffices – the change in porosity due to compaction only affects the reservoir pressure negligibly. We employed a linear-elastic model for the subsurface response, with the compacting blocks in the reservoir as source terms [Fokker and Orlic, 2006]. Using an influence function approach, the subsidence at any surface point then is a superposition of

the contributions of all compacting reservoir blocks. For the elastic profile in the subsurface we used a homogeneous elastic modulus down to a rigid basement at a depth of 5000 m. The reservoir is located at a depth of 3000 m. The connection to the double differences measured with the optical leveling can be made by making the appropriate time differences combined with space differences.
The goal of the present study was to employ an inverse algorithm on the interpreted double differences to improve the history match of the reservoir model and the predictive capability of the model in terms of reservoir pressures and subsidence. We considered the compaction of the reservoir as the uncertain parameter – the reservoir pressures and the porosities underlying it would involve too large computational efforts for this assessment. To map the uncertainty of the reservoir compaction we employed a field of multiplication factors at a spacing of 3200 m in space and 4 years in time. Values at the actual grid and intermediate times were obtained by interpolation. The prior multiplication values were defined as a constant value of unity over the field. A standard deviation of 0.3 was assumed. The mathematics of development

Inverse model

For the inverse model we define the vector **m** as the collection of adjustable model parameters, the vector **d** as the collection of double-difference data, and the matrix **G**, working on the model parameters, as the forward model. The inverse problem is then formulated as the task of estimating the vector $\hat{\mathbf{m}}$ for which $\mathbf{G}\hat{\mathbf{m}}$ approaches the data vector **d** best. With additional information present in the form of a prior model ($\mathbf{m}_0$) and covariance matrices of the measurements ($\mathbf{C}_d$) and of the prior model ($\mathbf{C}_m$), the conventional least-squares solution is obtained by maximizing the objective function J given by Tarantola [2005] (or by minimizing $-\log[J]$):

$$J = \exp\left[-\frac{1}{2}(\mathbf{m}-\mathbf{m}_0)^T\mathbf{C}_m^{-1}(\mathbf{m}-\mathbf{m}_0) - \frac{1}{2}(\mathbf{d}-\mathbf{Gm})^T\mathbf{C}_d^{-1}(\mathbf{d}-\mathbf{Gm})\right]$$

For the linear problem at hand, the estimate and its covariance are given by

$$\begin{aligned}\hat{\mathbf{m}} &= \mathbf{m}_0 + \mathbf{C}_m\mathbf{G}^T(\mathbf{G}\mathbf{C}_m\mathbf{G}^T+\mathbf{C}_d)^{-1}(\mathbf{d}-\mathbf{G}\mathbf{m}_0)\\ &= \mathbf{m}_0 + (\mathbf{G}^T\mathbf{C}_d^{-1}\mathbf{G}+\mathbf{C}_m^{-1})^{-1}\mathbf{G}^T\mathbf{C}_d^{-1}(\mathbf{d}-\mathbf{G}\mathbf{m}_0)\\ \mathbf{C}_{\hat{\mathbf{m}}} &= \mathbf{C}_m - \mathbf{C}_m\mathbf{G}^T(\mathbf{G}\mathbf{C}_m\mathbf{G}^T+\mathbf{C}_d)^{-1}\mathbf{G}\mathbf{C}_m\\ &= (\mathbf{G}^T\mathbf{C}_d^{-1}\mathbf{G}+\mathbf{C}_m^{-1})^{-1}\end{aligned}$$

in which the first or second line of both expressions can be chosen according to the number of data points and model parameters [Tarantola, 2005]. A smoothness constraint was added by extending the data vector with a number of elements equal to the number of multipliers in the model parameters, and by assigning the Laplacian working on **m** as the forward model for those elements. Furthermore, an independent constant vertical velocity for every benchmark was used as an additional unknown parameter to allow for movement not caused by the depletion of the gas field.

Results

The inversion exercise yielded an update of the fields of multiplication values and values for the autonomous movement of the benchmarks. With the original unit values and with the expected values of the multiplication factors, the forward model was rerun. Figure 2 shows the prior and posterior calculated double differences against the measured values. Although the scatter is still large, there is a clear improvement. The quality of the fit, indicated by $\chi^2 = \frac{1}{N}(\mathbf{Gm}-\mathbf{d})^2/\sigma_d^2$, improved from 8.8 to 5.9 – the first and second number being calculated with the prior and the

estimated model parameters, respectively. The remaining value around 6, much larger than an optimal value around 1, is presumably related to a remaining instability in the selected benchmarks, however it could also mean that the standard deviation of the height difference is too optimistic. The average of the background movement of the benchmark is zero; the standard deviation is 0.5 mm/year.
There is a clear effect on the compaction fields. Examples of prior and updated compaction fields are given in Fig. 3. They show that around some areas the compaction levels must be adjusted to explain the measurements. These areas consistently return, independent of variations of the amount of smoothing or the precise form of the influence function in the forward model. More compaction than assumed in the prior model seems to have taken place around Ten Boer [(x_{RD}; y_{RD}) = (243,000; 588,000)]; less around Delfzijl [(x_{RD}; y_{RD}) = (255,000; 592,000) and less around Uithuizen [(x_{RD}; y_{RD}) = (245,000; 605,000)]. The improvement of the double difference estimates and the effect on the subsidence estimates benchmarks is represented in Figs. 4 and 5.

Discussion

The correlation between measured and predicted double differences is much better for the estimated values of the multiplication factors than for the prior values. Still, the scatter remains considerable and there are many points with estimated value around zero that show comparatively large measured double differences. In view of this, it is remarkable that the inversion results in a consistent increase of compaction around Ten Boer and consistent decreases around Delfzijl and Uithuizen. This result was even apparent when no background movement was taken into account and the resulting correlation between measured and predicted double difference values was even worse. We assume that instabilities of individual benchmarks will cause deviations of double differences connected to them which are compensated with deviations with opposite sign for double differences starting from them.
Independent support for the updated compaction field has been found in a separate study [Van Thienen-Visser and Breunese, 2015]. In that study, a different forward compaction model was employed and the predicted surface subsidence was compared to differences of interpreted heights at stable benchmarks and PS-InSAR measurement of the surface movement velocity. The areas that we found here were also identified in that study, and an additional effort was already recommended there to improve the subsurface model in those areas as it pointed towards inaccuracies of the porosity model and the assumed aquifer activity.

Conclusions

The present study proves the possibility of using double differences of optical levelling between stable benchmarks for the determination of reservoir parameters by its application on the Groningen gas field. The inverse study that we performed yielded a consistent update of the compaction of Groningen gas field during the lifetime of the field. The area around Ten Boer is compacting more than in the prior compaction model; the areas around Delfzijl and Uithuizen less. This is consistent with independent results obtained from comparing predicted subsidence with temporal differences of interpreted benchmark elevations. A renewed effort of reservoir modelling is required to improve the understanding of the reservoir in these areas.

References

Fokker, P. A. and Van Thienen-Visser, K.:. On the use of double differences in inversion of surface movement measurements. Paper ARMA 15-096, presented at the 49th US Rock Mechanics / Geomechanics Symposium. San Francisco, CA, USA, 28 June – 1 July 2015.

Tarantola: Inverse Problem Theory and Methods for Model Parameter Estimation. SIAM, Paris, France, 2005

Van Thienen-Visser, K and Breunese, J.N.: Induced seismicity of the Groningen gas field: history and recent developments. The Leading Edge, special issue Injection Induced Seismicity, 2015, *in press.*

Van Thienen-Visser, K., Pruiksma, J and Breunese, J.N.: Compaction and Subsidence of the Groningen gas field in the Netherlands. Submitted to NISOLS, 2015

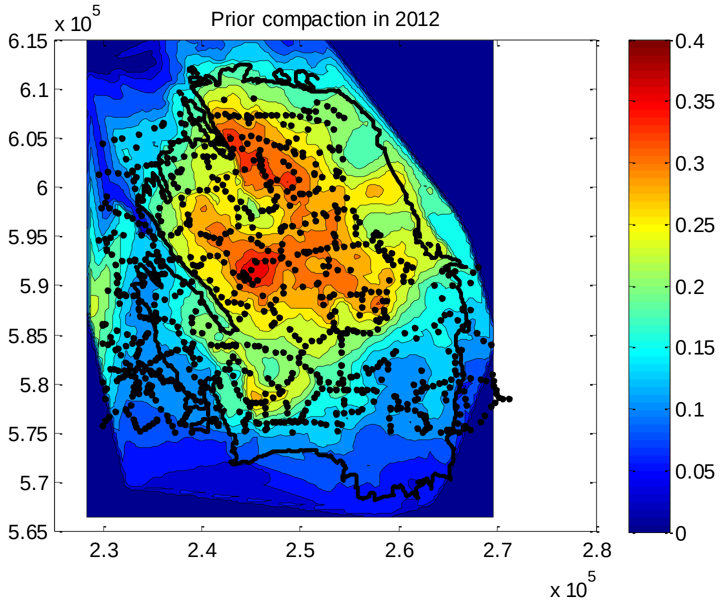


Figure 1 Prior estimate of the compaction field of the Groningen gas field in 2012 (color-coded), outline of the gas-bearing layers (solid line) and surface locations of the benchmarks used in the study (filled dots).

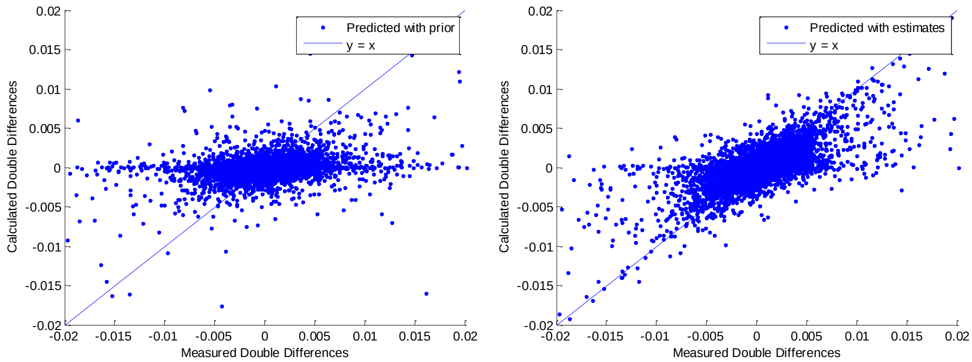


Figure 2 Predicted versus measured double differences, predicted with prior compaction field (left) and with estimated compaction field allowing point noise (right).

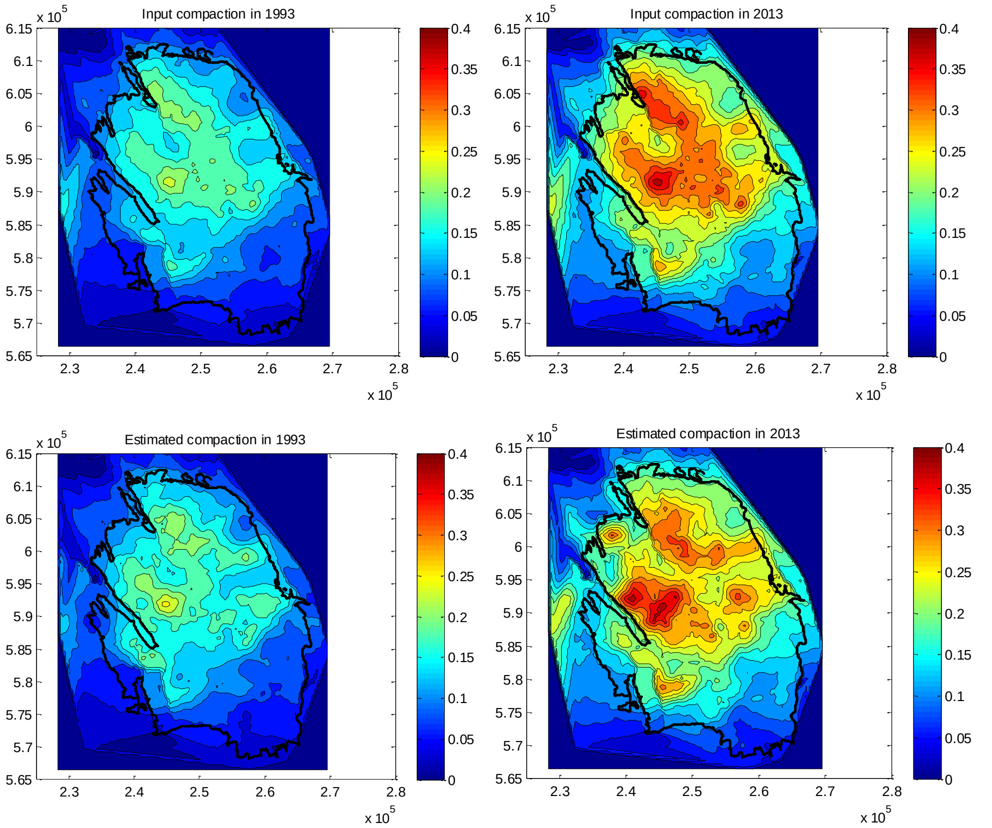


Figure 3 Prior compaction fields (top row) and estimated compaction fields (bottom row) in 1993 (left) and in 2013 (right)

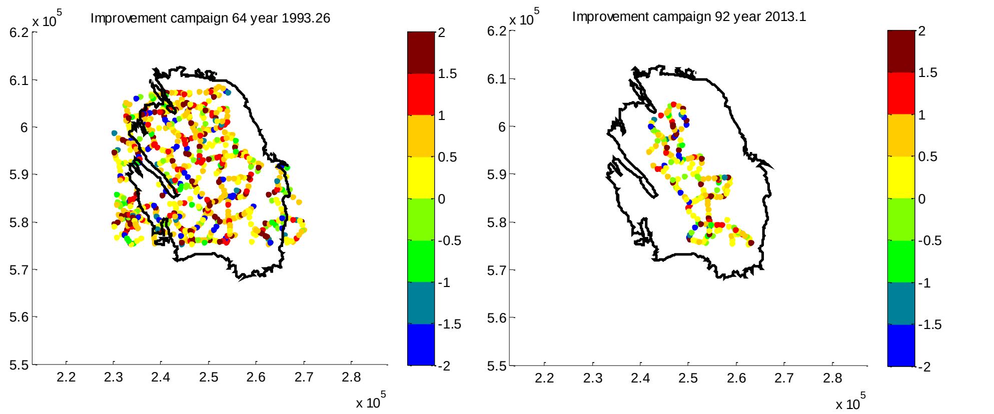


Figure 4 Improvement of the fit of double differences measured for two out of the 92 campaigns – towards 1993 and 2013 (starting times are variable for the different points). The color code indicates the ratio between prior and posterior offset: $(\mathbf{Gm}_E - \mathbf{d})/(\mathbf{Gm}_0 - \mathbf{d})$. Absolute values of this number smaller than 1 (yellow or green) indicate improvement.

B Introduction theory to Bayesian Point Change Model

In this appendix the Bayesian Point Change Model is explained. The Bayesian Point Change model takes a Bayesian approach to the retrospective analysis of a Poisson process with a single change point at an unknown time. The rate of occurrence at time s, $\alpha(s)$, is equal to α_1 if $0 \leq s \leq \tau$ and α_2 if $s > \tau$ .The analysis is based on the observation period $[0, T]$, during which *n* events occur at times $t = (t_{1,} t_{2,} \dots, t_n)$. The variables τ, α_1, α_2 represent the date of change, event occurrence rate before the change, and occurrence rate after the change, respectively.

We assume that τ, α_1, α_2 are independent a priori, and that the prior densities of α_1 and α_2 have the conjugate form:

$$p(\alpha_j) \propto \alpha_j^{k_j - 1} e^{-\alpha_{j/\theta_j}}$$

The likelihood is

$$\mathcal{L}(\tau, \alpha_1, \alpha_2 | t) = \prod_{t=t_1}^{t_\tau} \alpha_1 e^{-\alpha_1 t} \prod_{t=t_\tau+1}^{t_n} \alpha_2 e^{-\alpha_2 t}$$
$$= \alpha_1^{N(\tau)} e^{-\tau\alpha_1} \alpha_2^{N(T)-N(\tau)} e^{-(T-\tau)\alpha_2}$$

where $N(t)$ is the number of events that occurred in the interval $[0, t]$. Thus, posterior density can be calculated as

$$p(\tau, \alpha_1, \alpha_2 | t) \propto \mathcal{L}(\tau, \alpha_1, \alpha_2 | t)\, p(\alpha_1) p(\alpha_2) p(\tau) \qquad (3),$$

since all parameters are mutually independent.
The marginal distribution for each of τ, α_1, and α_2 can thus be obtained by integrating the posterior density over the remaining two variables. The posterior density of τ is thus

$$p(\tau | t) = p(\tau) \int_0^\infty \alpha_1^{N(\tau)+k_1-1} e^{-\left(\tau + \frac{1}{\theta_1}\right)\alpha_1} d\,\alpha_1$$
$$\int_0^\infty \alpha_2^{N(t)-N(\tau)+k_2-1} e^{-\left(T-\tau+\frac{1}{\theta_2}\right)\alpha_2} d\,\alpha_2$$
$$= \frac{1}{T} \frac{\Gamma(r_1(\tau))\, \Gamma(r_2(\tau))}{S_1(\tau)^{r_1(\tau)}\, S_2(\tau)^{r_2(\tau)}}$$

where $r_1(\tau) = N(\tau) + k_1$
$S_1(\tau) = \tau + \frac{1}{\theta_1}$
$r_2(\tau) = N(T) - N(\tau) + k_2$
$S_2(\tau) = T - \tau + \frac{1}{\theta_2}$

Furthermore,

$$p(\tau) = \frac{1}{T}, \quad 0 \leq \tau \leq T$$

since the prior distribution for the time of change τ is assumed to be uniformly distributed over the observation period. This means that the change in event rate is equally likely to occur at any time during that period.

The posterior density of the event rate before the change α_1 is obtained by integrating equation 3 over τ and α_2. This does not yield a simple analytic form. The function is discontinuous in τ. The most convenient form for numerical integration is the sum of integrals of some continuous functions. Therefore, the time range is discretized on a daily basis, and summed to approximate the marginal posterior distribution.

$$p(\alpha_1|\tau) \approx \sum_{\tau=0}^{T}\left[\frac{1}{T}\ \alpha_1^{r_1(\tau)-1} e^{-\alpha_1 S_1(\tau)} \Gamma\big(r_2(\tau)\big) S_2(\tau)^{r_2(\tau)}\right]$$

The posterior distribution of event rate after the change point, can be calculated in a similar way:

$$p(\alpha_2|\tau) \approx \sum_{\tau=0}^{T}\left[\frac{1}{T}\ \alpha_2^{r_2(\tau)-1} e^{-\alpha_2 S_2(\tau)} \Gamma\big(r_1(\tau)\big) S_1(\tau)^{r_1(\tau)}\right]$$

Bayes factor

The test for a change point compares a model with a change point to a model with a constant event rate. The change point model is applied to the observed data assuming that there is a change point. It calculates the probability of change on any given date. To actually check whether the data support the presence of a change rate or favours the model with the constant event rate, a Bayes factor is used (see also TNO 2014b).
The Bayes factor β is defined as the ratio of the likelihood function for a constant rate model H_0 to that of a change model H_1. The constant rate model has only one unknown parameter, which is a constant rate of occurrence (i.e., constant seismic event rate). For conjugate priory of constant rate the same gamma distribution is used:

$$p(\alpha_0) \ \propto\ \alpha_j^{k_0}\ e^{-\alpha_0/\theta_0}$$

leading to likelihood function:

$$\mathcal{L}(\ H_0|t) = \int_0^{\infty} \mathcal{L}(\alpha_0|t)\ p(\alpha_0) d\alpha_0$$

and similarly for the change model to:

$$\mathcal{L}(\ H_1|t) = \int_0^{T}\int_0^{\infty}\int_0^{\infty} \mathcal{L}\big(\tau,\alpha_{1,}\alpha_2\big|t\big)\ p(\alpha_1)p(\alpha_2)p(\tau)\ d\alpha_1\, d\alpha_2\, d\tau$$

If the value of parameters for gamma conjugate priors are $k_j = 0.5$ and $\theta_j \to \infty$ for $j = 0{,}1{,}2$ then it is shown by Raftery and Akman (1986) that the equation for Bayes factor can be simplified to:

$$\beta(t) = 4\sqrt{\pi}\, T^{-n}\, \Gamma(n+1/2)\ \left[\sum_{\tau=0}^{T} \Gamma\big(r_1(\tau)\big) S_1(\tau)^{-r_1(\tau)}\, \Gamma\big(r_2(\tau)\big) S_2(\tau)^{-r_2(\tau)}\right]^{-1}$$

When the Bayes factor is small enough (less than 1) it means that the change point model is supported by the data. In this study, a change point model is favoured if the Bayes factor is smaller than 0.001. Every time a change point is foundthe data strongly support a change point model. If, on the other hand, a change point is not found (Bayes factor > 0.001); than this means that the constant model is preferred.

In the case of a small number of events, the constant model is automatically preferred above the change point model.

References

Gupta, A., and J. Baker: A Bayesian change point model to detect changes in event occurrence rates, with application to induced seismicity, *12th international Conference on Applications of Statistics and Probability* in Civil Engineering ICASP12, Vancouver, Canada, July 12-15, 2015.

Raftery, A. and V. Akman: Bayesian analysis of a Poisson process with a change-point. *Biometrika,*73(1), 85-89, 1986.